

- Supporting Information -

**Synthesis and Characterisation of Halide, Separated Ion Pair, and Hydride Cyclopentadienyl Iron Bis(Diphenylphosphino)ethane Derivatives**

Dipti Patel,<sup>1</sup> Ashley Wooles,<sup>1</sup> Andrew D. Cornish,<sup>1</sup> Lindsey Steven,<sup>1</sup> E. Stephen Davies,<sup>1</sup> David J. Evans,<sup>\*2</sup> Jonathan McMaster,<sup>1</sup> William Lewis,<sup>1</sup> Alexander J. Blake,<sup>1</sup> and Stephen T. Liddle<sup>\*1</sup>

<sup>1</sup> School of Chemistry, University of Nottingham, University Park, Nottingham, NG7 2RD, UK.

<sup>2</sup> Department of Chemistry, University of Hull, Hull, HU6 7RX, UK.

\*email: stephen.liddle@nottingham.ac.uk; david.evans@hull.ac.uk

**Electrochemistry**

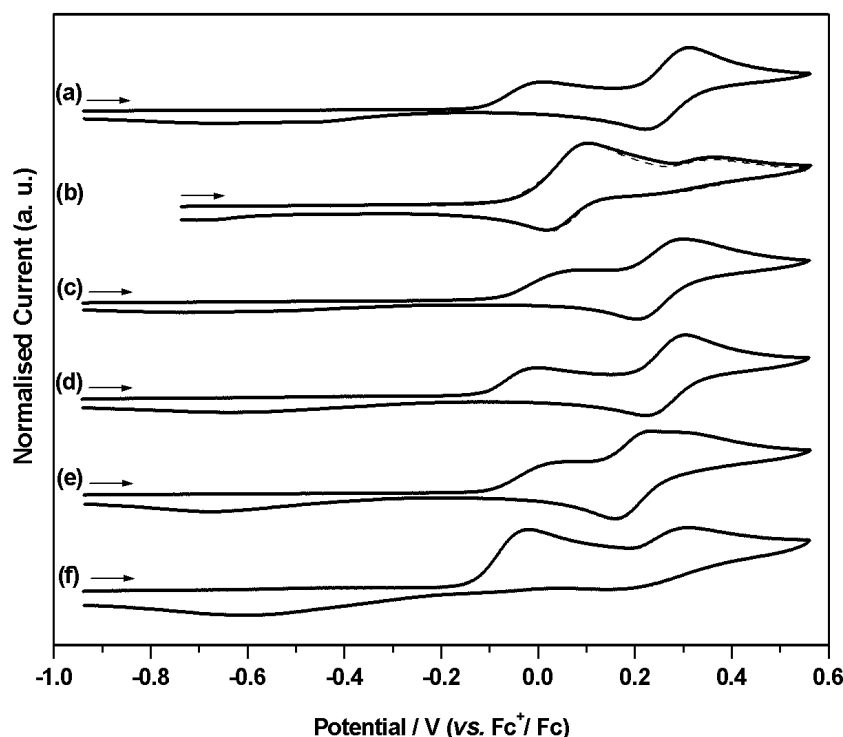


**Figure S1:** Cyclic voltammograms for (a)  $[Fe(Cp)(l)(dppe)]$ , (b)  $[Fe(Cp^*)(l)(dppe)]$  (solid line) and 2SIP (dashed line), (c)  $[Fe(Cp')(l)(dppe)]$ , (d)  $[Fe(Cp'')(l)(dppe)]$ , (e)  $[Fe(Cp'')^t(l)(dppe)]$  and (f)  $[^nBu_4N][I]$  in MeCN containing  $[NBu_4]^+[BF_4]^-$  (0.1 M) as supporting electrolyte at  $0.1\text{ Vs}^{-1}$ . Currents are normalised to  $I_p^a$  for clarity. Typical currents obtained from CV experiments for the separated ion pairs in MeCN are shown in Figure SI3 for 2SIP, as are designations of OX, OX', OX'' and RED for 1SIP-5SIP used in Table SII.

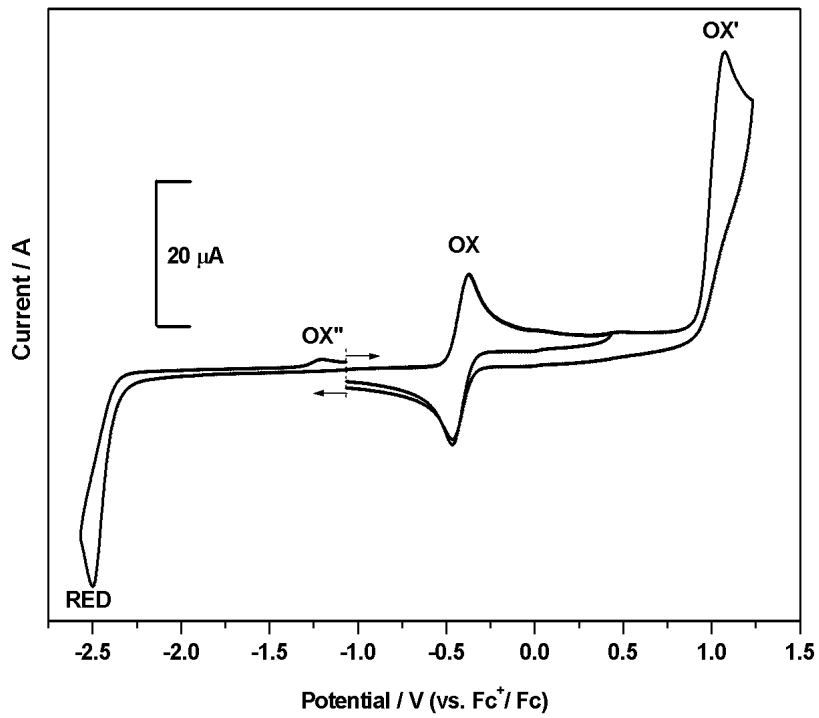


**Figure S2a:** Cyclic voltammetry for  $[\text{Fe}(\text{Cp}')(\text{Cl})(\text{dppe})]$  in THF containing  $[\text{NBu}_n]^+ \text{BF}_4^-$  (0.5 M) as supporting electrolyte, at  $0.1 \text{ Vs}^{-1}$ , showing designations of OX, OX', OX'' and RED for **1Cl-5Cl**, **1Br-5Br**, **1I-5I** and **1H-5H** compounds used in Table SII.

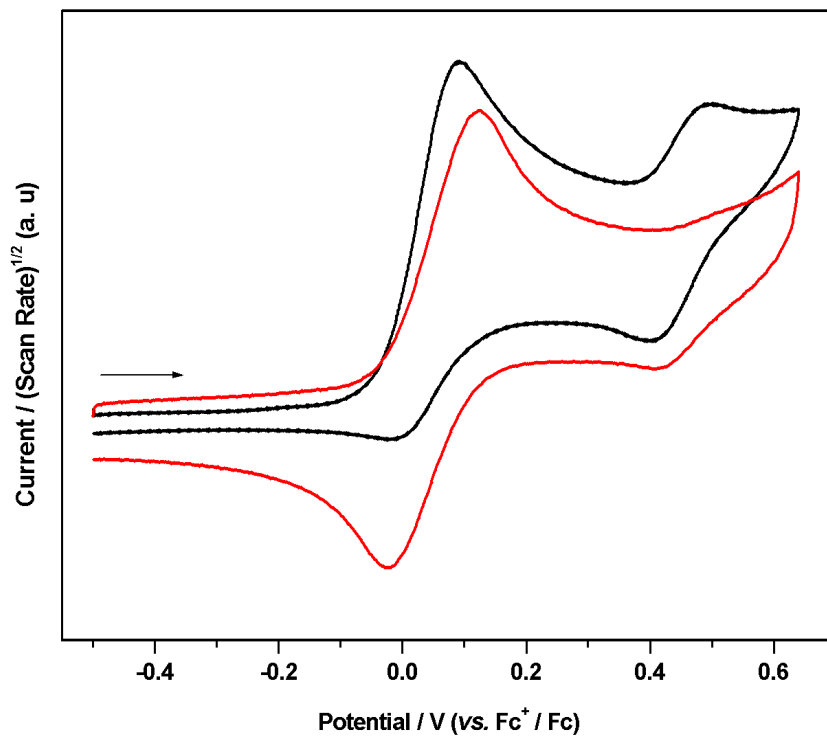


**Figure S2b:** Cyclic voltammetry for compound **4H** in THF containing  $[\text{NBu}_n]^+ \text{BF}_4^-$  (0.5 M) as supporting electrolyte, at  $0.1 \text{ Vs}^{-1}$  (black line) and  $1.0 \text{ Vs}^{-1}$  (red line). Note that the oxidation process at  $E_p^a + 0.49 \text{ V}$  is scan rate dependent, and is diminished as OX becomes reversible at faster scan rate.

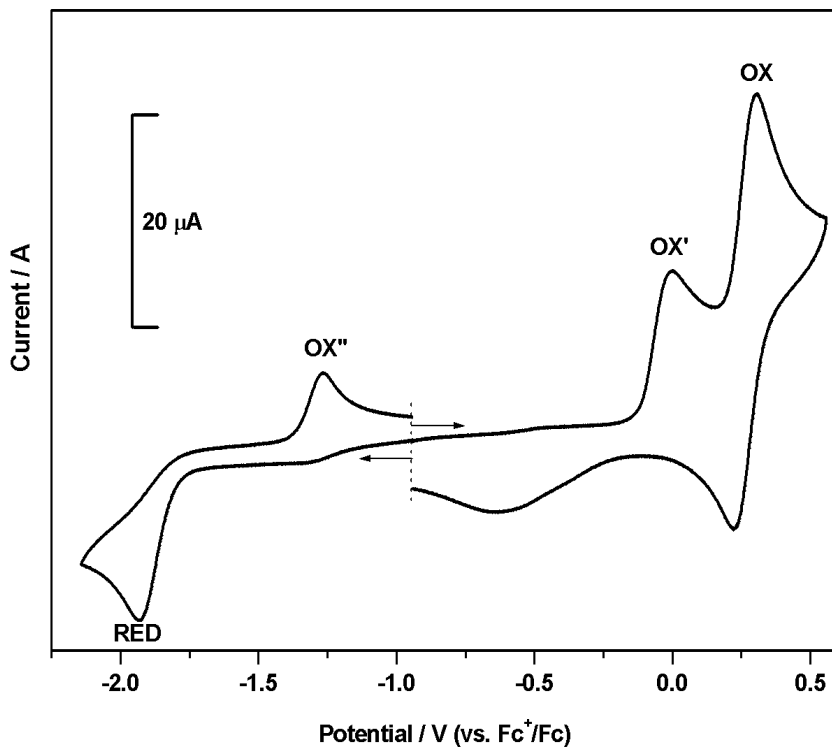


**Figure S3:** Cyclic voltammetry for  $[\text{Fe}(\text{Cp}^\dagger)(\text{I})(\text{dppe})]$  in MeCN containing  $[\text{NBu}_4]^+[\text{BF}_4]^-$  (0.1 M) as supporting electrolyte, at  $0.1 \text{ Vs}^{-1}$ , showing designations of OX, OX', OX'' and RED for **1SIP-5SIP** compounds used in Table SII.

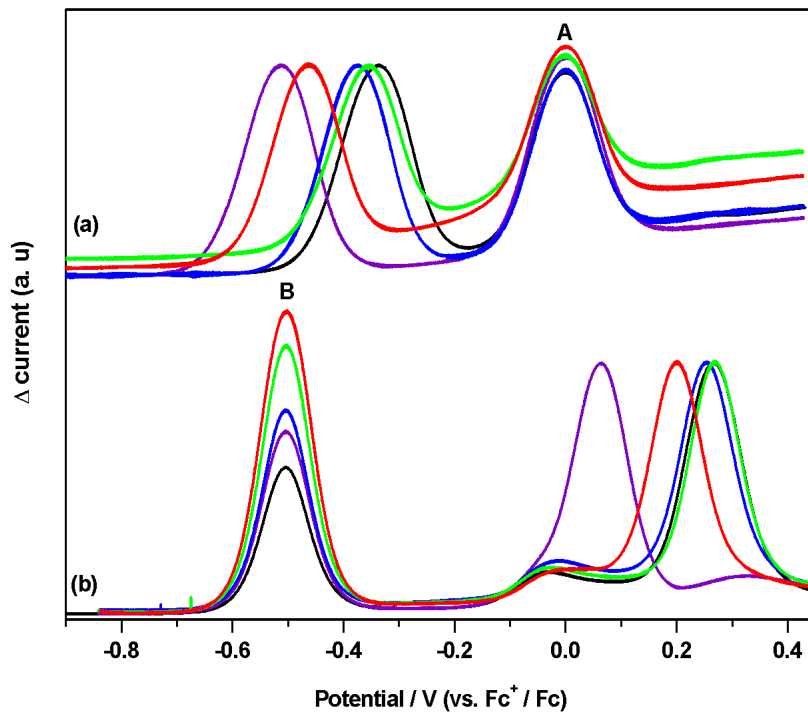


**Figure S4:** Square wave voltammetry showing OX for (a)  $[\text{Fe}(\text{Cp}^\dagger)(\text{Cl})(\text{dppe})]$  in THF containing  $[\text{NBu}_4]^+[\text{BF}_4]^-$  (0.5 M) as supporting electrolyte and (b)  $[\text{Fe}(\text{Cp}^\dagger)(\text{I})(\text{dppe})]$  in MeCN containing  $[\text{NBu}_4]^+[\text{BF}_4]^-$  (0.1 M) as supporting electrolyte ( $\text{Cp}^\dagger = \text{Cp}$  (black),  $\text{Cp}^*$  (violet),  $\text{Cp}'$  (blue),  $\text{Cp}''$  (green),  $\text{Cp}'''$  (red)). The peaks labelled A and B are ferrocene and decamethylferrocene, respectively used as the internal standards.

	<b>OX</b> $E_{1/2}$ / V <sup>a</sup>	$\Delta Fc^b$	$-I_p^c/I_p^{a\ c}$	$I_p$ vs. (scan rate) <sup>1/2</sup> ( $R^2$ ) <sup>d</sup>	Square wave / V	<b>OX'</b> ( $E_p^a$ ) / V	<b>RED</b> ( $E_p^c$ ) / V	<b>OX''</b> ( $E_p^a$ ) / V
<b>1Cl</b>	-0.42 (0.09)	(0.10)	1.03	1.000, 0.998	-0.42	+1.08	-2.50	-1.20
<b>1Br</b>	-0.38 (0.10)	(0.10)	1.05	1.000, 0.997	-0.38	+1.12	-2.49	-1.20
<b>1I</b>	-0.34 (0.09)	(0.10)	1.04	0.999, 0.997	-0.34	+1.09 <sup>g</sup>	-2.32(sh), -2.48	-1.21
<b>1H</b>	-0.50 (0.09)	(0.09)	1.03	1.000, 0.994	-0.51	+0.73	-	-
<b>1SIP<sup>f</sup></b>	+0.26 (0.09)	(0.07)			+0.27	-0.01	-2.10	-
<b>2Cl</b>	-0.59 (0.10)	(0.10)	0.99	0.999, 0.999	-0.59	+0.87 <sup>h</sup>	-2.64	-1.29
<b>2Br</b>	-0.55 (0.09)	(0.09)	0.96	0.999, 0.999	-0.55	+0.95 <sup>g</sup>	-2.55	-1.30
<b>2I</b>	-0.51 (0.09)	(0.10)	1.02	0.998, 0.998	-0.51	+0.81 <sup>i</sup>	-2.42(sh), -2.57	-1.29
<b>2H</b>	-0.71 (0.09)	(0.10)	1.05	0.999, 0.991	-0.71	+0.57	-	-
<b>2SIP<sup>f</sup></b>	+0.06 (0.09)	(0.07)			+0.06	-	-2.20	-
<b>3Cl</b>	-0.45 (0.09)	(0.10)	1.01	1.000, 0.997	-0.45	+0.51 <sup>p</sup>	-2.49	-1.10
<b>3Br</b>	-0.41 (0.09)	(0.10)	1.04	0.999, 0.996	-0.41	+1.06	-2.49	-1.10
<b>3I</b>	-0.37 (0.09)	(0.09)	1.00	0.998, 0.998	-0.37	+0.99 <sup>j</sup>	-2.51	-1.07
<b>3H</b>	-0.50 (0.09)	(0.09)	0.84	0.994, 0.985	-0.50	+0.56 <sup>g</sup>	-	-
<b>3SIP<sup>f</sup></b>	+0.25 (0.1)	(0.07)			+0.25	+0.01	-2.05	-1.33
<b>4Cl</b>	-0.44 (0.09)	(0.10)	0.96	0.996, 0.998	-0.44	+0.51 <sup>k</sup>	-2.47	-1.01
<b>4Br</b>	-0.40 (0.09)	(0.10)	0.91	0.996, 0.999	-0.39	-	-2.50 <sup>l</sup>	-1.01
<b>4I</b>	-0.36 (0.10)	(0.10)	1.06	0.996, 0.999	-0.35	+0.38	-2.26, -2.47 <sup>m</sup>	-1.03
<b>4H</b>	-0.53 (0.15) <sup>e</sup>	(0.16)	-	0.955, -	-0.50	-	-	-
<b>4SIP<sup>f</sup></b>	+0.26 (0.08)	(0.07)			+0.27	0.00	-1.93	-1.27
<b>5Cl</b>	-0.54 (0.08)	(0.09)	0.77	0.992, 0.974	-0.54	-0.10 <sup>p</sup>	- <sup>n</sup>	-1.07 <sup>p</sup>
<b>5Br</b>	-0.50 (0.09)	(0.09)	0.76	0.998, 0.983	-0.51	+0.54	-1.85 <sup>p</sup>	-1.10 <sup>p</sup>
<b>5I</b>	-0.46 (0.09)	(0.09)	0.89	0.999, 0.996	-0.46	-	- <sup>o</sup>	-
<b>5H</b>	-0.62 (0.09)	(0.09)	1.05	0.998, 0.999	-0.62	+0.77	-	-
<b>5SIP<sup>f</sup></b>	+0.20 (0.08) <sup>q</sup>	(0.07)			+0.20	+0.06	-2.05	-1.31

**Table S1:** <sup>a</sup> In THF containing  $[NBu^4_4][BF_4]$  (0.5 M) as supporting electrolyte. At ambient temperature. Potentials quoted against  $E_{1/2} Fc^+/Fc$  at 0.10  $Vs^{-1}$  used as the internal standard unless stated otherwise. Values in brackets are  $\Delta E$  ( $= E_p^a - E_p^c$ );  $E_{1/2} = (E_p^a + E_p^c)/2$ ;  $E_p^a$  = peak anodic (oxidation) potential;  $E_p^c$  = peak cathodic (reduction) potential. <sup>b</sup>  $\Delta Fc = E_p^a - E_p^c$  for the  $Fc^+/Fc$  couple at 0.10  $Vs^{-1}$ . <sup>c</sup> at 0.1  $Vs^{-1}$ . <sup>d</sup> from data recorded at 0.1, 0.2, 0.3, 0.05 and 0.02  $Vs^{-1}$ ,  $R^2$  values for  $I_p^a$  and  $I_p^c$ , respectively. <sup>e</sup> at 1.00  $Vs^{-1}$  and  $[CoCp_2][PF_6]$  used as the internal standard to avoid overlap of couples. Potential quoted against the  $Fc^+/Fc$  couple using an independent calibration where  $E_{1/2} [CoCp_2]^+/[CoCp_2] = -1.359$  V vs.  $Fc^+/Fc$  under identical conditions. <sup>f</sup> In MeCN containing  $[NBu^4_4][BF_4]$  (0.1 M) as supporting electrolyte and  $[Fe(\eta^5-$

$C_5Me_5)_2]$  used as the internal standard to avoid overlap of couples. Potentials quoted against the  $Fc^+/Fc$  couple using an independent calibration where  $E_{1/2} [Fe(\eta^5-C_5Me_5)_2]^+ / [Fe(\eta^5-C_5Me_5)_2] = -0.505 V$  vs.  $Fc^+/Fc$  under identical conditions. Current analysis not performed due to the presence of overlapping iodide electrochemistry. <sup>g</sup> increase in current but not resolved as a well-defined peak. <sup>h</sup> return wave noted for this oxidation process in reduction half-cycle:  $E_{1/2} +0.81 V (0.13)$  ( $\Delta Fc 0.12$ ) at  $0.3 Vs^{-1}$ . <sup>i</sup> return wave noted for this oxidation process in reduction half-cycle:  $E_{1/2} +0.76 V (0.13)$  ( $\Delta Fc 0.13$ ) at  $0.3 Vs^{-1}$ . <sup>j</sup> return wave noted for this oxidation process in reduction half-cycle:  $E_{1/2} +0.94 V (0.11)$  at  $0.1 Vs^{-1}$  ( $E_{1/2} +0.94 V (0.12)$  ( $\Delta Fc 0.12$ ) at  $0.3 Vs^{-1}$ ). <sup>k</sup> small couple noted at  $E_{1/2} +0.09 V (0.08)$ . <sup>l</sup> a small return wave was associated with this reduction at  $E_p^a -2.37 V$ . <sup>m</sup> return wave noted for this reduction process in oxidation half-cycle:  $E_{1/2} +2.42 V (0.10)$  at  $0.1 Vs^{-1}$ . <sup>n</sup> no defined peak but small current noted at potentials more cathodic than ca.  $-1.15 V$ . <sup>o</sup> asymmetric couple noted  $E_p^c -1.22 V$  (broad)  $E_p^a -1.11 V$  (sharp) at  $0.1 Vs^{-1}$ . <sup>p</sup> small feature. <sup>q</sup> overlaps with an additional feature at  $E_p^a +0.36 V$ .

## DFT Experimental and Supplementary Information

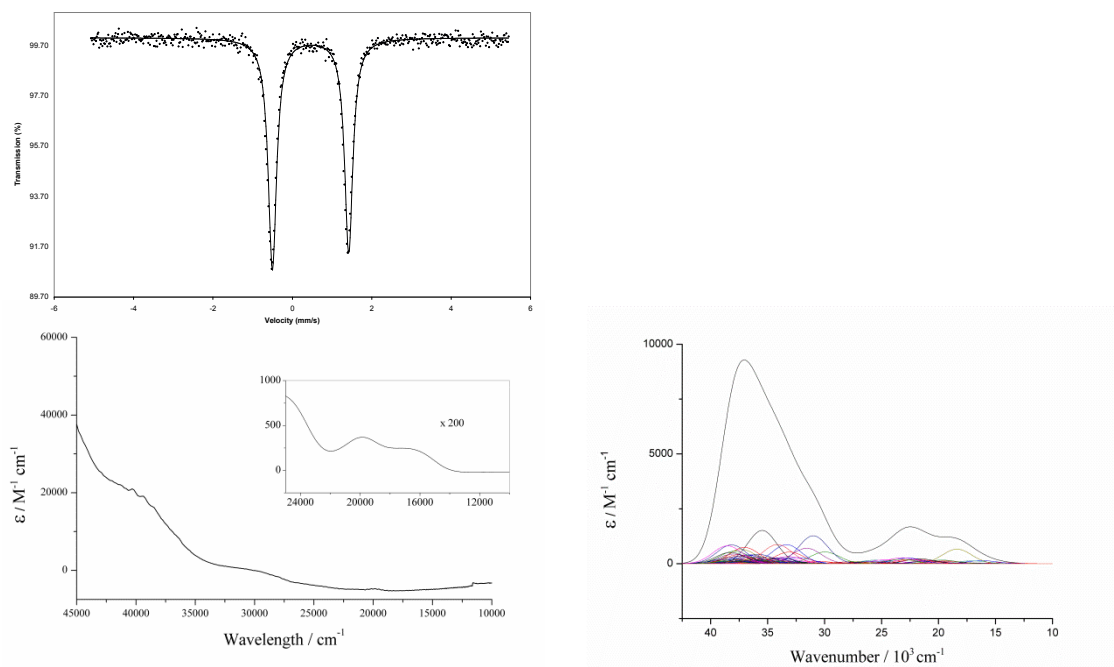
Compound	Fe1-Ct	Fe1-Cl1	Fe1-P1	Fe1-P2	Ct-Fe1-Cl1	Cl1-Fe1-P1	Cl1-Fe1-P2
<b>1Cl</b>	1.699(3) 1.711	2.3317(9) 2.343	2.1963(10) 2.191	2.1846(10) 2.181	123.9(9) 121.64	87.90(3) 88.73	89.11(3) 89.26
<b>2Cl</b>	1.732 1.744	2.346(1) 2.358	2.197(1) 2.202	2.210(1) 2.216	119.06 118.6	87.23(5) 87.47	86.03(4) 85.83
<b>3Cl</b>	1.716(5) 1.72	2.3298(16) 2.343	2.198(16) 2.202	2.1881(15) 2.186	123.8(19) 123.19	90.18(6) 88.96	86.15(6) 86.08
<b>4Cl</b>	1.704(7) 1.742	2.294(2) 2.348	2.184(2) 2.201	2.194(2) 2.213	121.24(2) 120.47	89.09(9) 89.57	87.64(8) 87.62
<b>5Cl</b>	1.739(4) 1.759	2.3423(10) 2.351	2.2358(10) 2.235	2.2107(11) 2.221	122.8(11) 121.48	89.18(4) 89.94	84.18(4) 85.08

**Table S2:** Representative comparison of experimental and theoretical bond lengths ( $\text{\AA}$ ) and angles ( $^\circ$ ) of **1Cl-5Cl** where Ct = centroid.

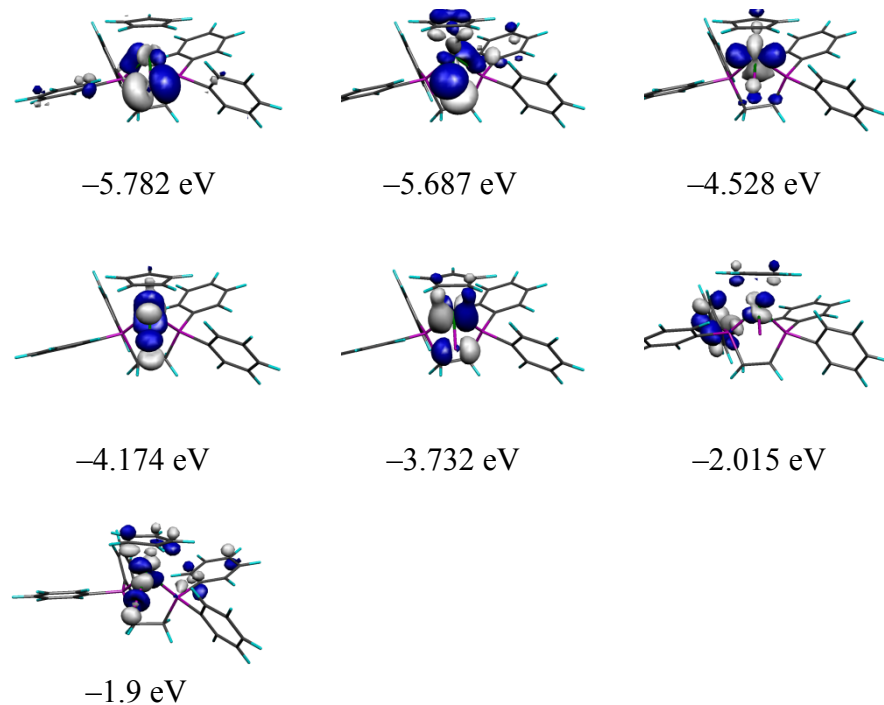
Compound	HOMO (eV)	Total Fe (%)	Fe s (%)	Fe p (%)	Fe d (%)	Total X (%)	X s (%)	X p (%)	X d (%)	Total Cp (%)	Cp s (%)	Cp p (%)	Cp d (%)	Total dppe (%)	dppe s (%)	dppe p (%)	dppe d (%)
<b>1Cl</b>	-3.73	70.23	0	0.95	69.28	14.35	0	13.95	0.40	9.38	0.04	8.93	0.41	6.04	1.05	3.96	1.02
<b>2Cl</b>	-3.53	72.68	0	0.80	71.88	11.11	0	10.70	0.41	10.13	1.60	7.98	0.53	6.09	0.82	4.18	1.09
<b>3Cl</b>	-3.69	70.06	0.04	0.84	69.18	13.22	0	12.82	0.41	10.45	0.19	9.64	0.62	6.27	0.92	4.34	1.01
<b>4Cl</b>	-3.74	69.14	0	0.73	68.41	12.02	0	11.63	0.39	12.42	0.41	11.18	0.83	6.44	0.88	4.51	1.04
<b>5Cl</b>	-3.54	73.07	0	0.83	72.24	12.29	0	11.88	0.41	9.15	0.42	8.30	0.43	5.48	0.74	3.79	0.95
<b>1Br</b>	-3.78	67.96	0	0.94	67.02	17.27	0	16.72	0.55	8.94	0.02	8.53	0.39	5.83	1.04	3.78	1.00
<b>2Br</b>	-3.56	72.00	0	0.83	71.19	13.44	0	12.88	0.57	9.46	1.43	7.53	0.50	5.10	0.69	3.42	1.00
<b>3Br</b>	-3.74	68.84	0.02	0.85	67.96	13.93	0	13.33	0.60	10.80	0.20	9.96	0.64	6.42	0.81	4.57	1.04
<b>4Br</b>	-3.78	67.29	0	0.75	66.55	13.69	0	13.13	0.56	12.58	0.46	11.29	0.84	6.43	0.82	4.58	1.04
<b>5Br</b>	-3.66	68.14	0	0.91	67.23	11.96	0	11.37	0.59	12.97	0.69	11.73	0.56	6.91	1.01	4.87	1.02
<b>1I</b>	-3.83	61.91	0	0.86	61.05	25.05	0	24.92	0.12	7.96	0.08	7.52	0.35	5.09	0.88	3.31	0.91
<b>2I</b>	-3.62	68.26	0	0.88	67.39	17.80	0	17.68	0.12	8.87	1.2	7.21	0.47	5.05	0.53	3.55	0.98
<b>3I</b>	-3.78	61.96	0.01	0.71	61.24	22.86	0	22.74	0.12	9.70	0.15	8.93	0.62	5.47	0.60	3.94	0.92
<b>4I</b>	-3.86	63.87	0.01	0.76	63.10	18.08	0	17.96	0.12	11.93	0.41	10.72	0.80	6.12	0.56	4.58	0.98
<b>5I</b>	-3.74	66.17	0	0.98	65.21	14.24	0	14.12	0.13	12.47	0.58	11.35	0.54	7.11	1.01	5.09	1.01
<b>1H</b>	-3.84	73.36	0.61	3.45	69.30	0.76	0.35	0.42	0	10.01	0.45	9.12	0.44	15.87	0.79	10.99	4.09
<b>2H</b>	-3.56	70.71	0.54	3.79	66.38	0.86	0.50	0.36	0	11.92	1.98	9.32	0.62	16.58	0.25	12.18	4.09
<b>3H</b>	-3.79	73.96	0.82	3.76	69.38	0.09	0.08	0.01	0	9.63	0.28	8.93	0.42	16.32	0.70	11.57	4.05
<b>4H</b>	-3.70	72.50	1.25	3.64	67.60	0.58	0.20	0.38	0	11.47	0.22	10.55	0.70	15.46	0.28	11.39	3.80
<b>5H</b>	-3.64	68.13	0.75	4.68	62.71	0.57	0.37	0.21	0	13.96	0.80	12.53	0.62	17.34	0.35	12.82	4.18

**Table S3:** Energies and compositions of the HOMO in **1Cl-5Cl**, **1Br-5Br**, **1I-5I** and **1H-5H**. Calculated using AOMix

**Analytical Data**  
**[Fe(Cp)(Cl)(dppe)], 1Cl**

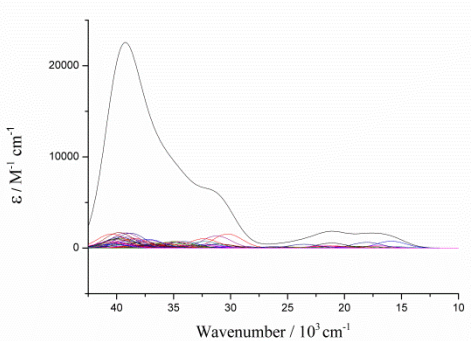
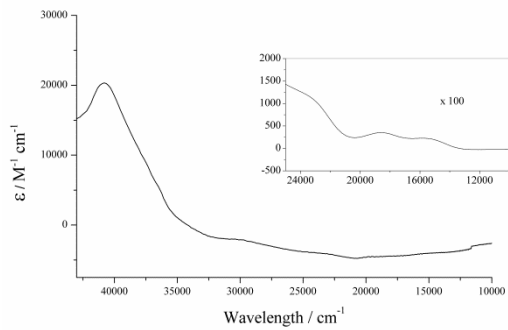
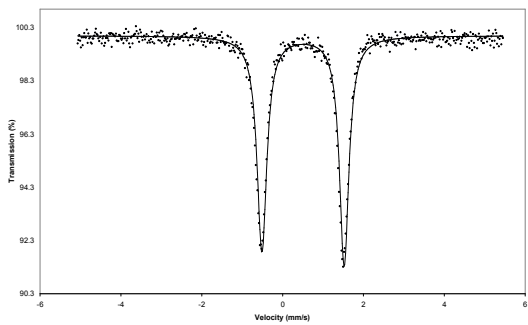


Top – Mossbauer  
 Bottom Left – Experimental UV-vis, Bottom Right – Calculated UV-vis



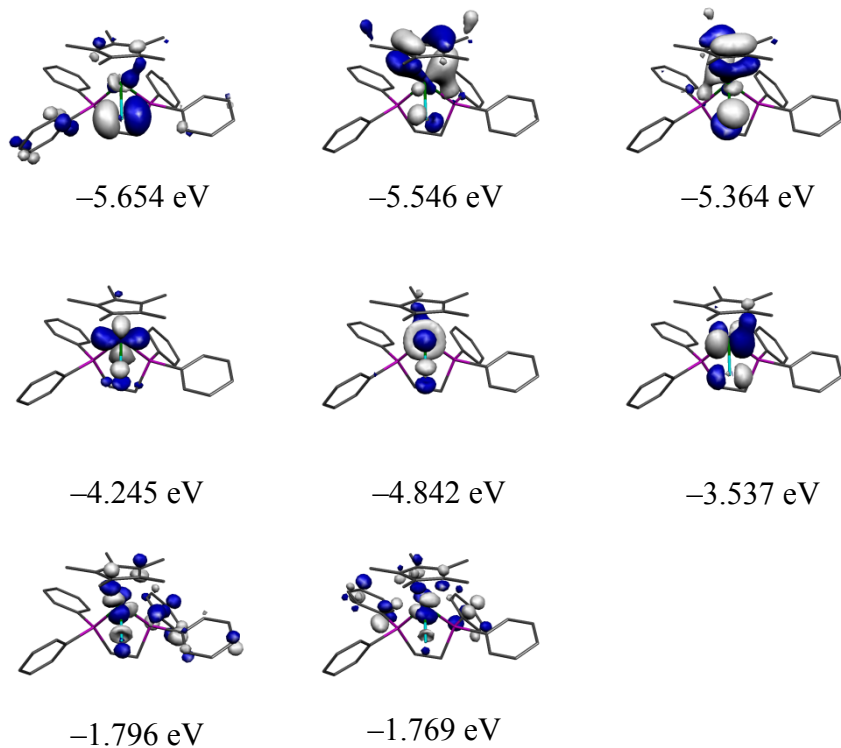
Kohn-Sham MO plots from HOMO-4 (top left) to LUMO+1 (bottom left)

**[Fe(Cp\*)(Cl)(dppe)], 2Cl**



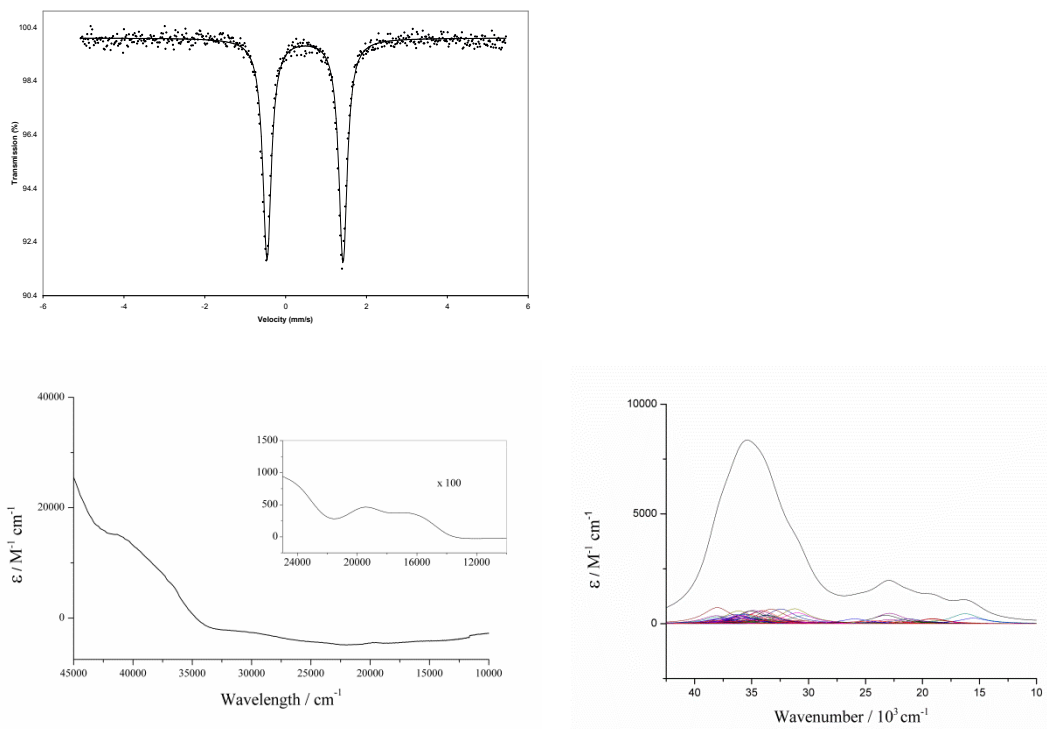
Top – Mossbauer

Bottom Left – Experimental UV-vis, Bottom Right – Calculated UV-vis



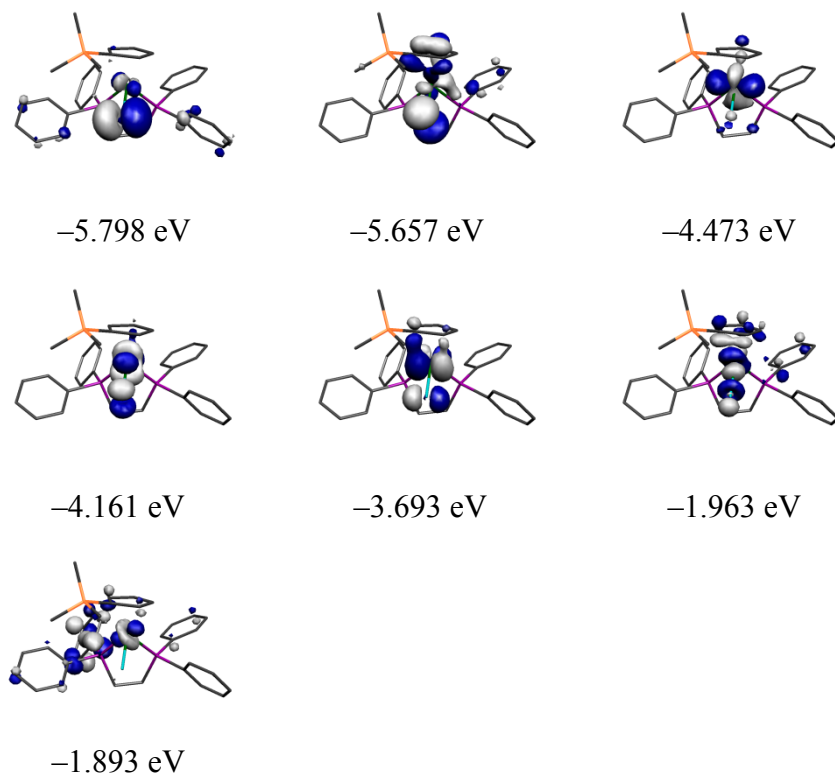
Kohn-Sham MO plots from HOMO-5 (top left) to LUMO+1 (bottom left)

**[Fe(Cp')(Cl)(dppe)], 3Cl**



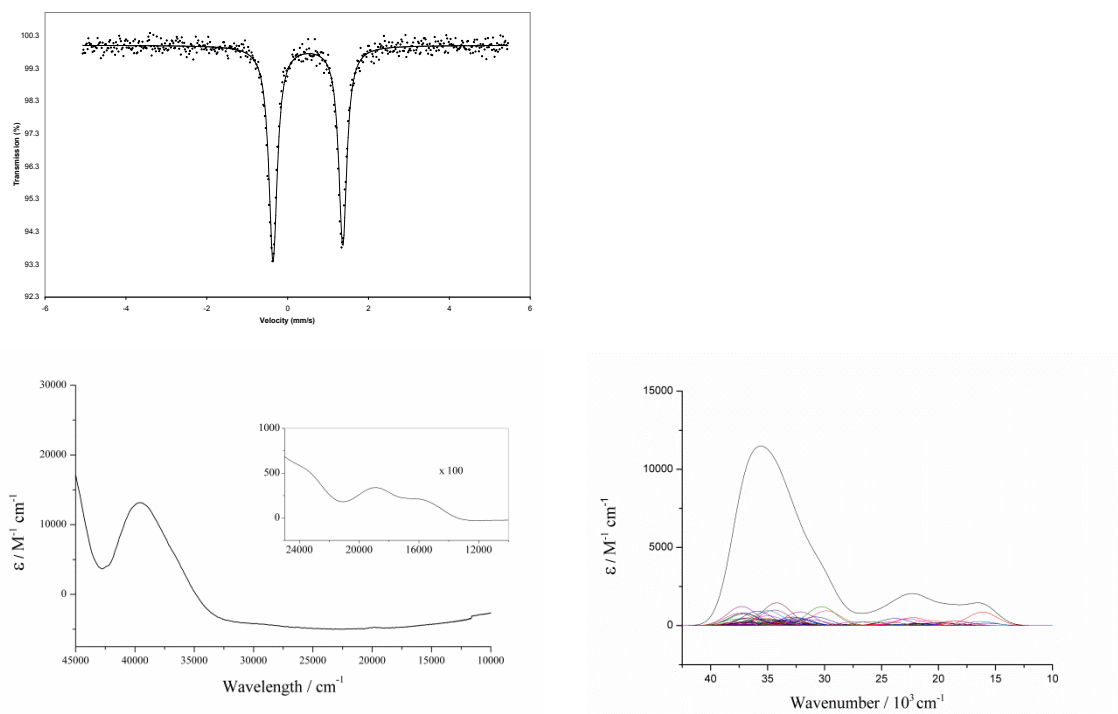
Top – Mossbauer

Bottom Left – Experimental UV-vis, Bottom Right – Calculated UV-vis



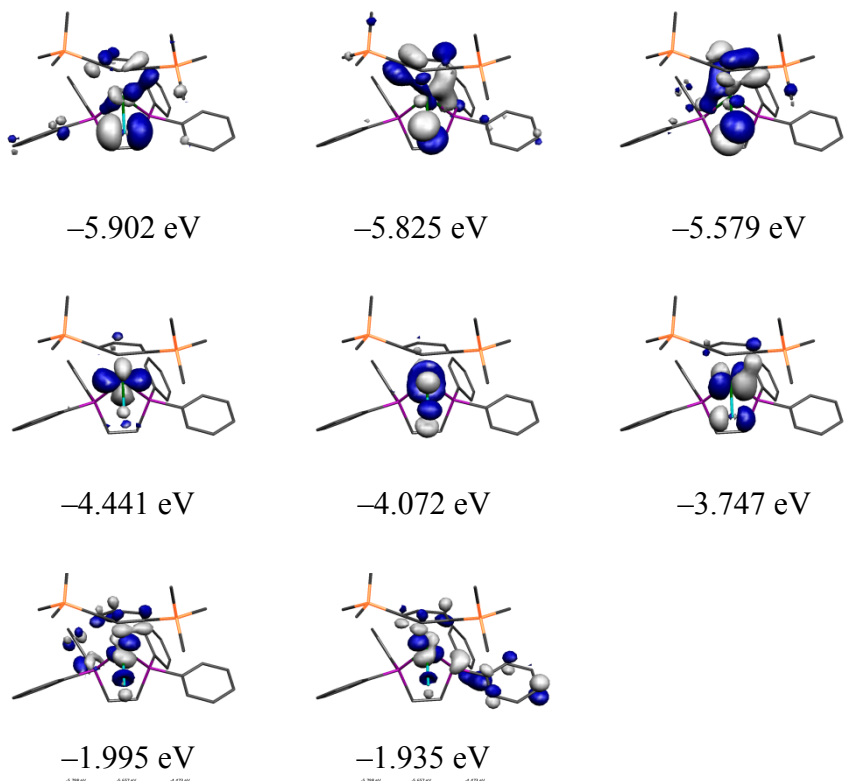
Kohn-Sham MO plots from HOMO-4 (top left) to LUMO+1 (bottom left)

**[Fe(Cp'')(Cl)(dppe)], 4Cl**



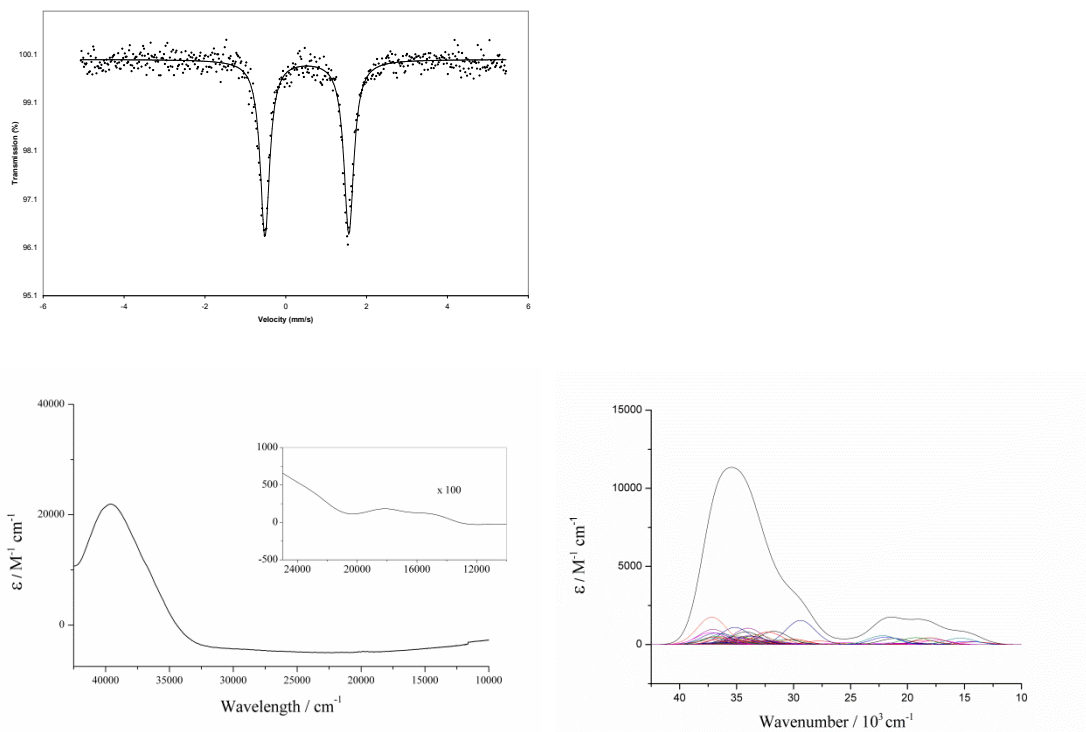
Top – Mossbauer

Bottom Left – Experimental UV-vis, Bottom Right – Calculated UV-vis



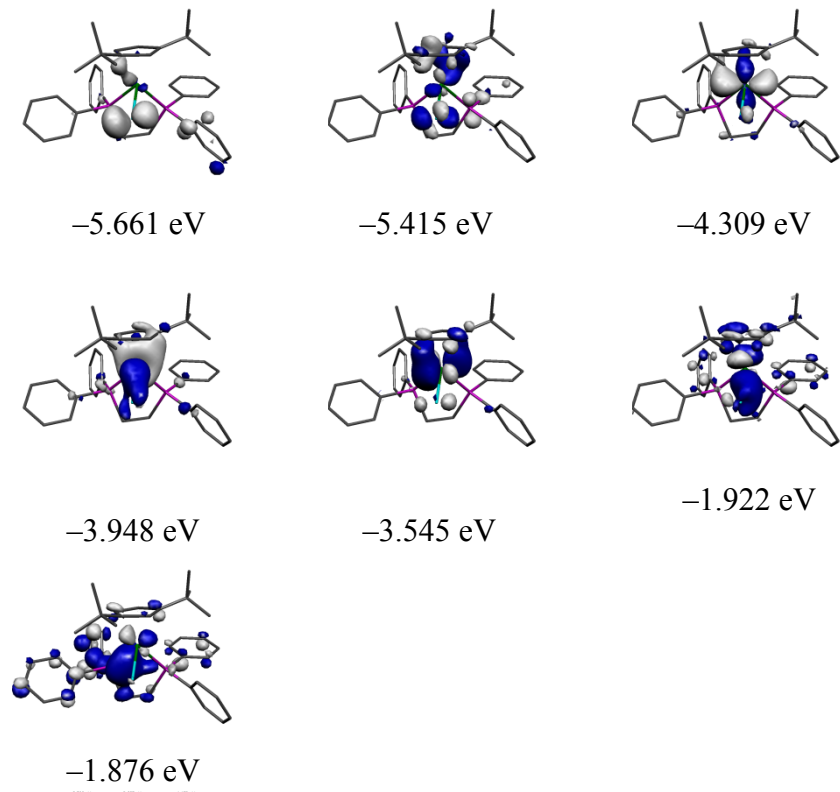
Kohn-Sham MO plots from HOMO-5 (top left) to LUMO+1 (bottom left)

**[Fe(Cp<sup>t</sup>)(Cl)(dppe)], 5Cl**



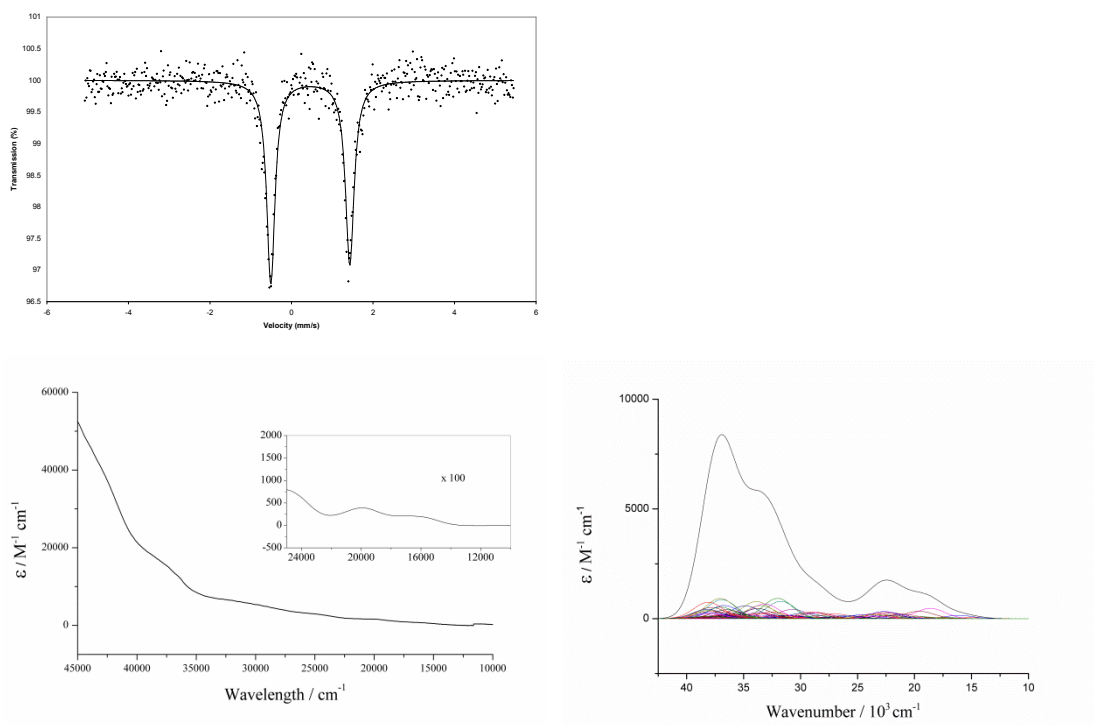
Top – Mossbauer

Bottom Left – Experimental UV-vis, Bottom Right – Calculated UV-vis



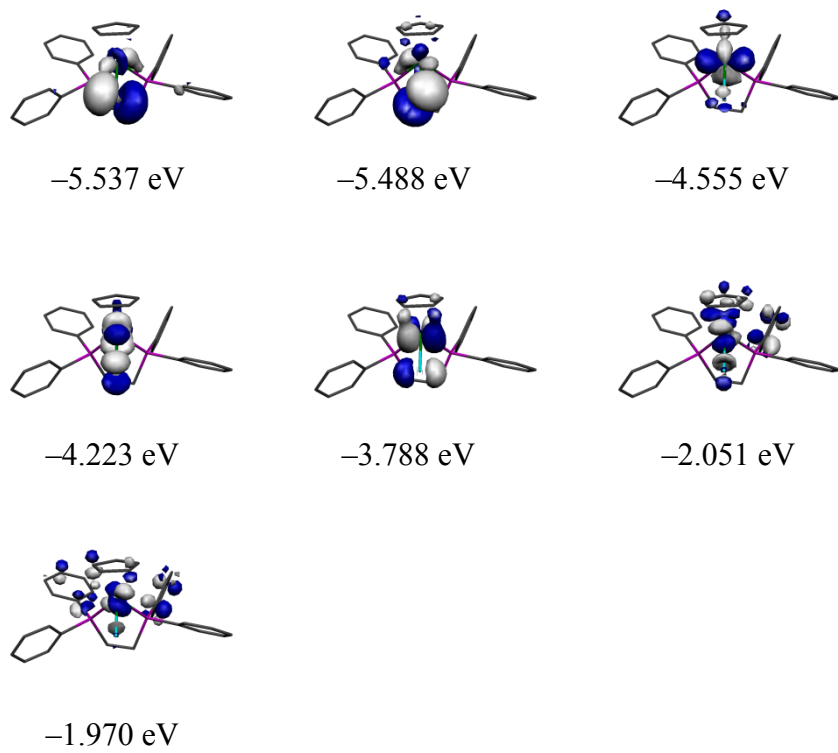
Kohn-Sham MO plots from HOMO-4 (top left) to LUMO+1 (bottom left)

**[Fe(Cp)(Br)(dppe)], 1Br**



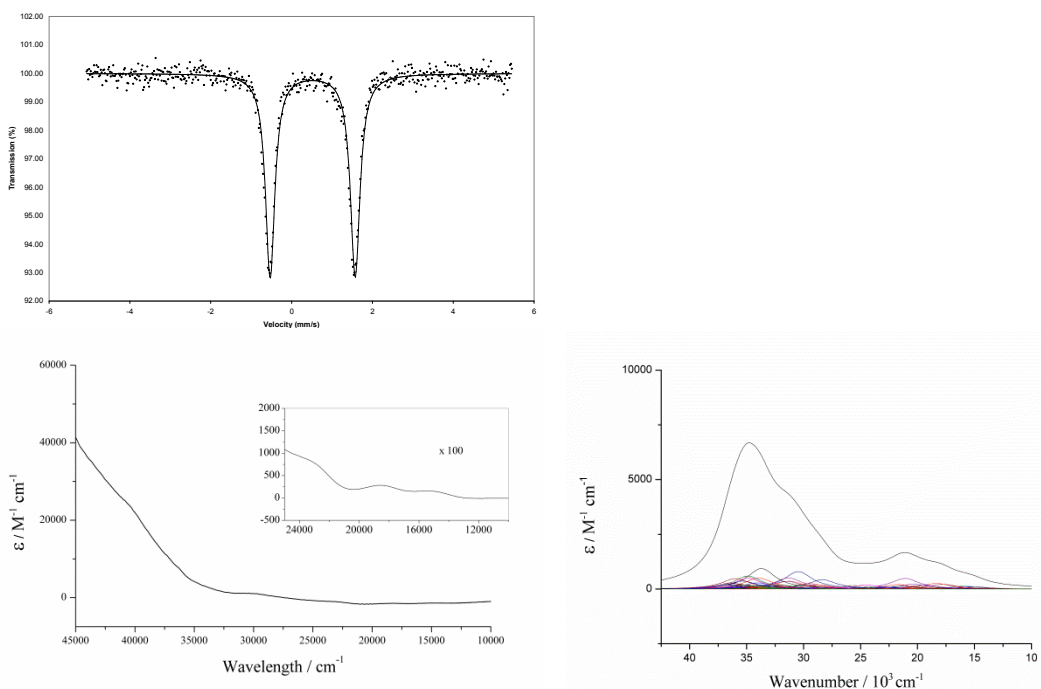
Top – Mossbauer

Bottom Left – Experimental UV-vis, Bottom Right – Calculated UV-vis



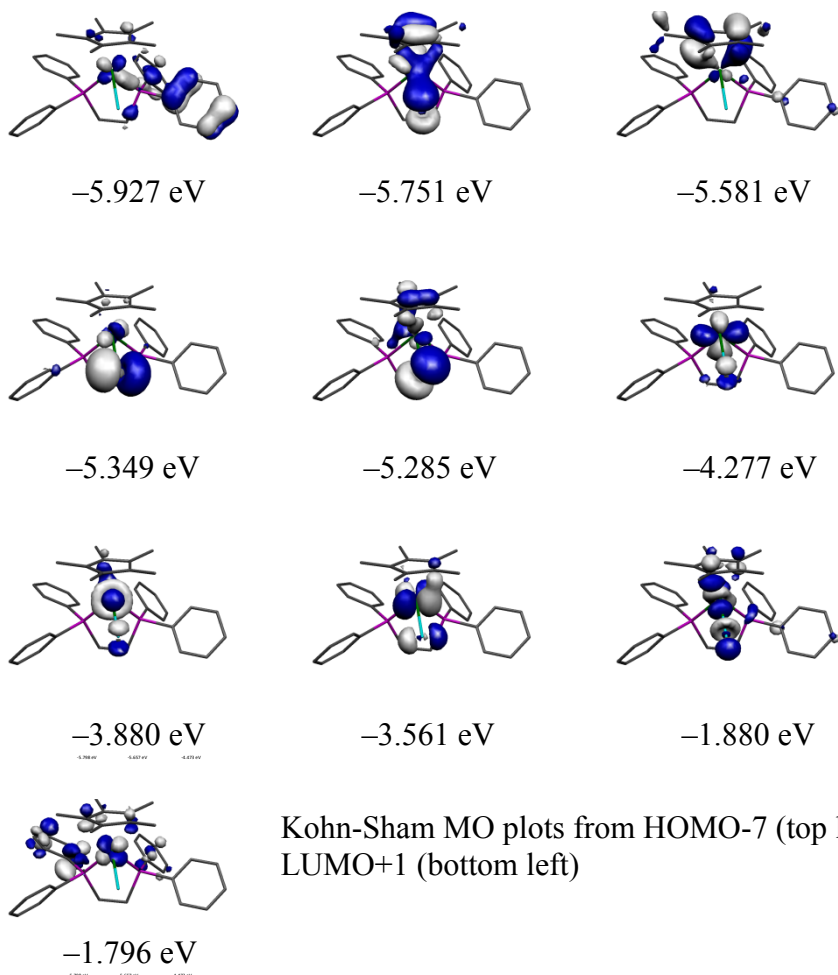
Kohn-Sham MO plots from HOMO-4 (top left) to LUMO+1 (bottom left)

**[Fe(Cp\*)(Br)(dppe)], 2Br**

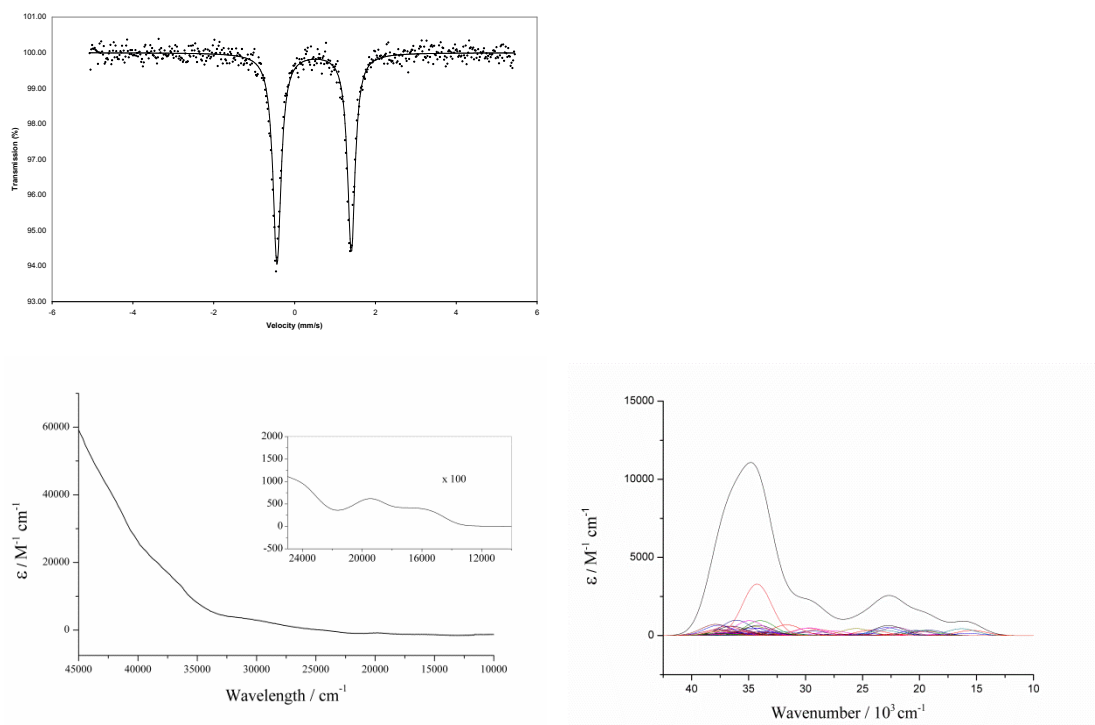


Top – Mossbauer

Bottom Left – Experimental UV-vis, Bottom Right – Calculated UV-vis

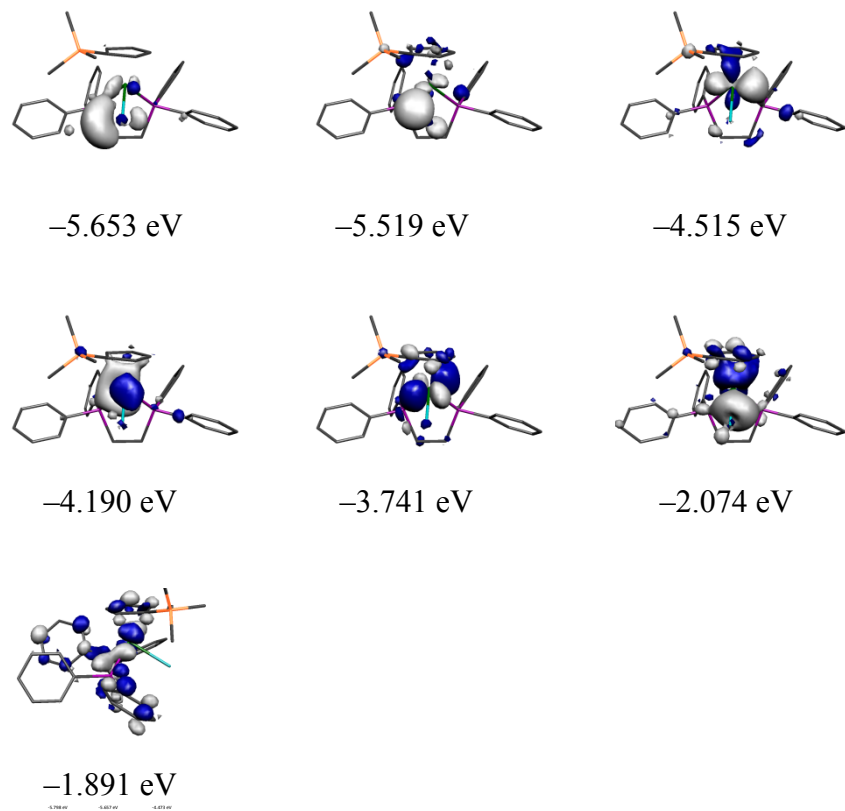


**[Fe(Cp')(Br)(dppe)], 3Br**



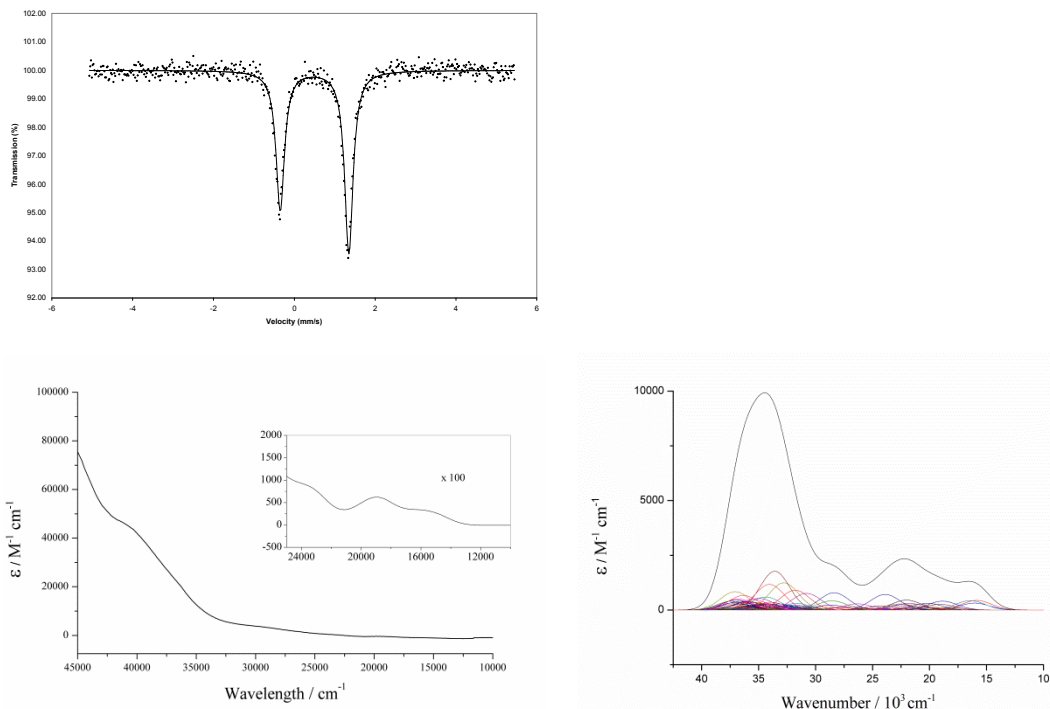
Top – Mossbauer

Bottom Left – Experimental UV-vis, Bottom Right – Calculated UV-vis



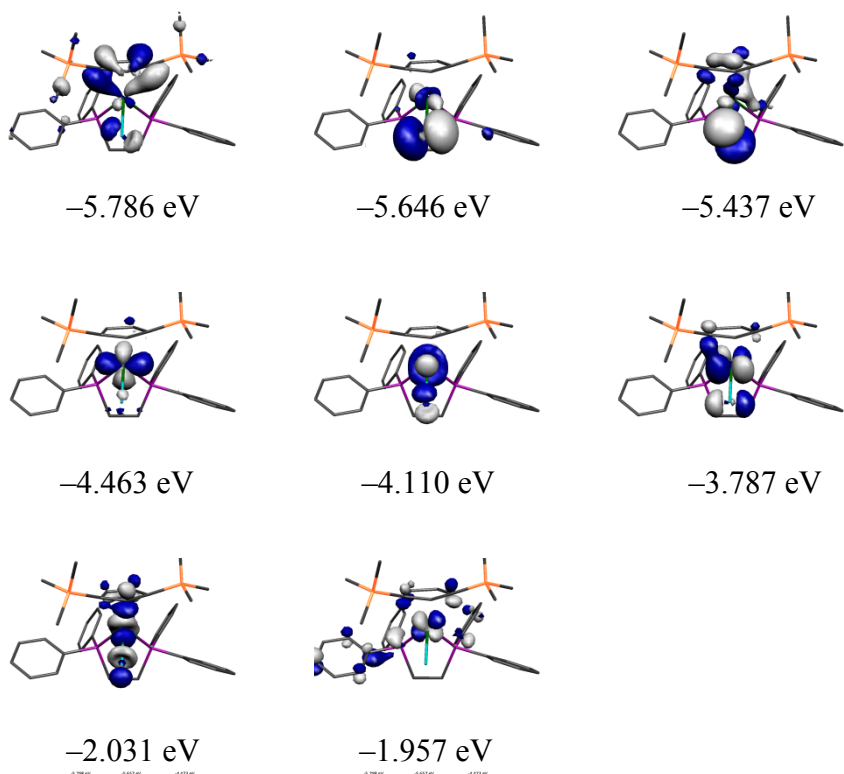
Kohn-Sham MO plots from HOMO-4 (top left) to LUMO+1 (bottom left)

**[Fe(Cp'')(Br)(dppe)], 4Br**



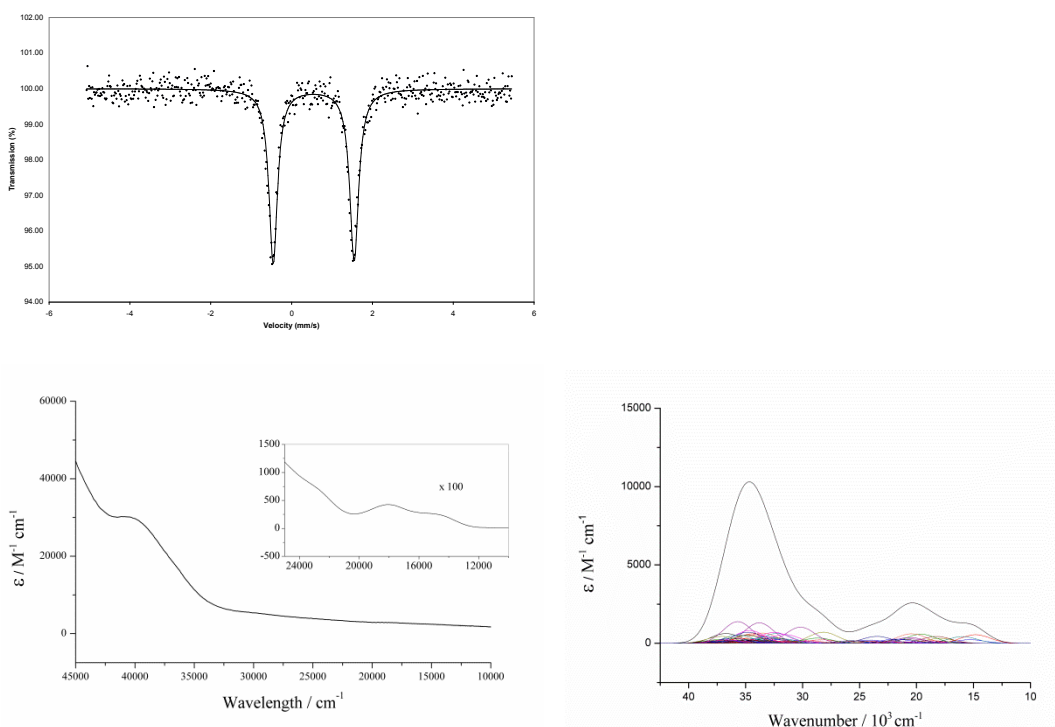
Top – Mossbauer

Bottom Left – Experimental UV-vis, Bottom Right – Calculated UV-vis



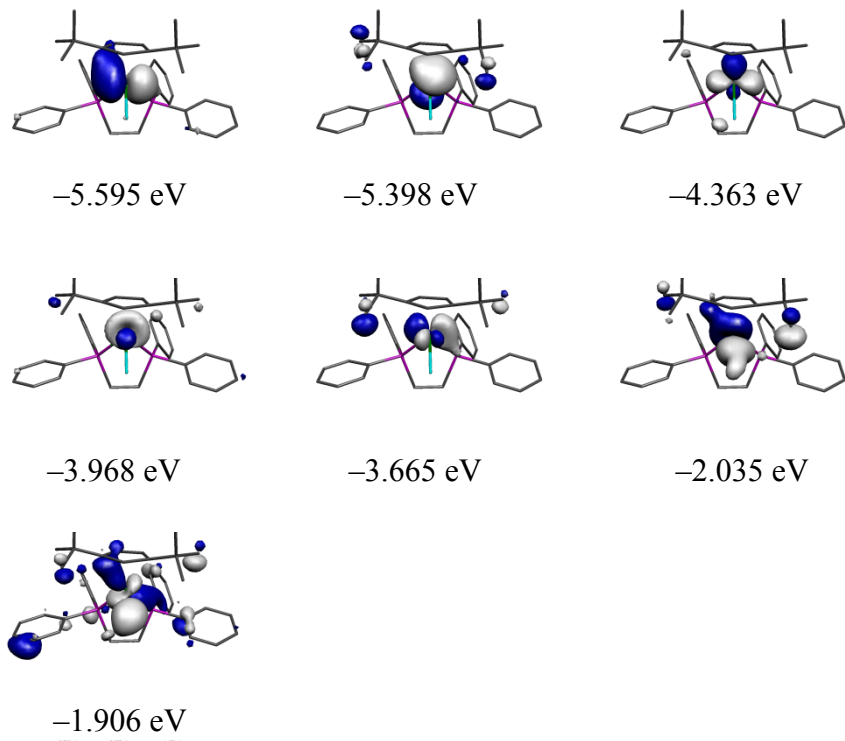
Kohn-Sham MO plots from HOMO-5 (top left) to LUMO+1 (bottom left)

**[Fe(Cp<sup>t</sup>)(Br)(dppe)], 5Br**



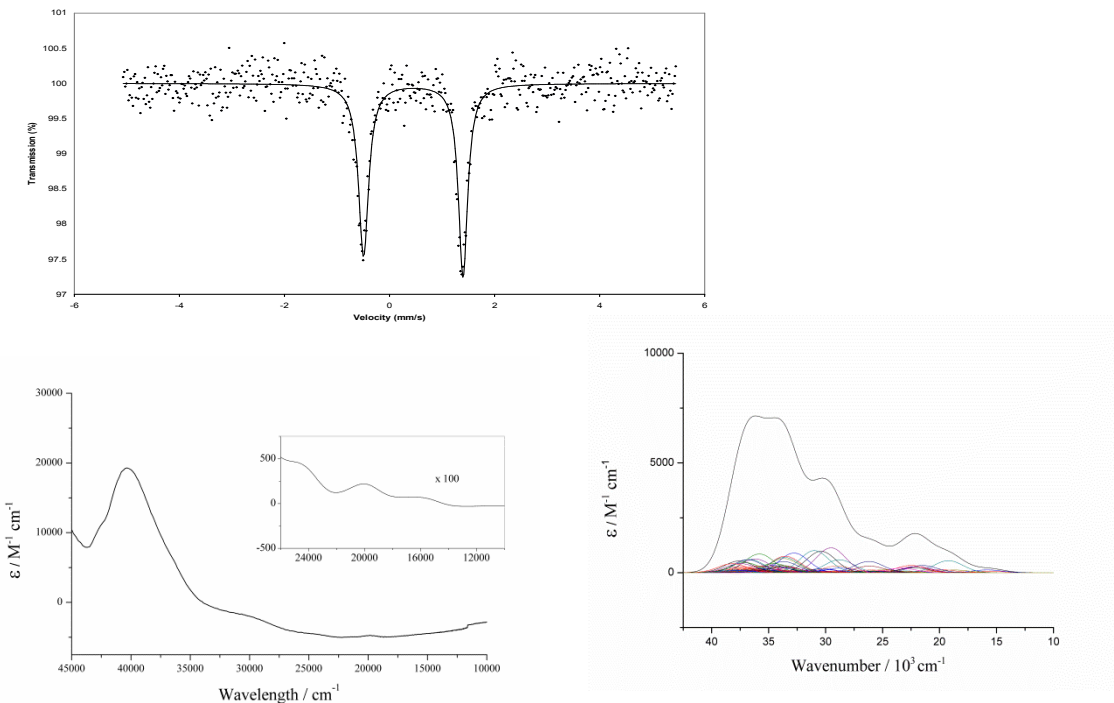
Top – Mossbauer

Bottom Left – Experimental UV-vis, Bottom Right – Calculated UV-vis



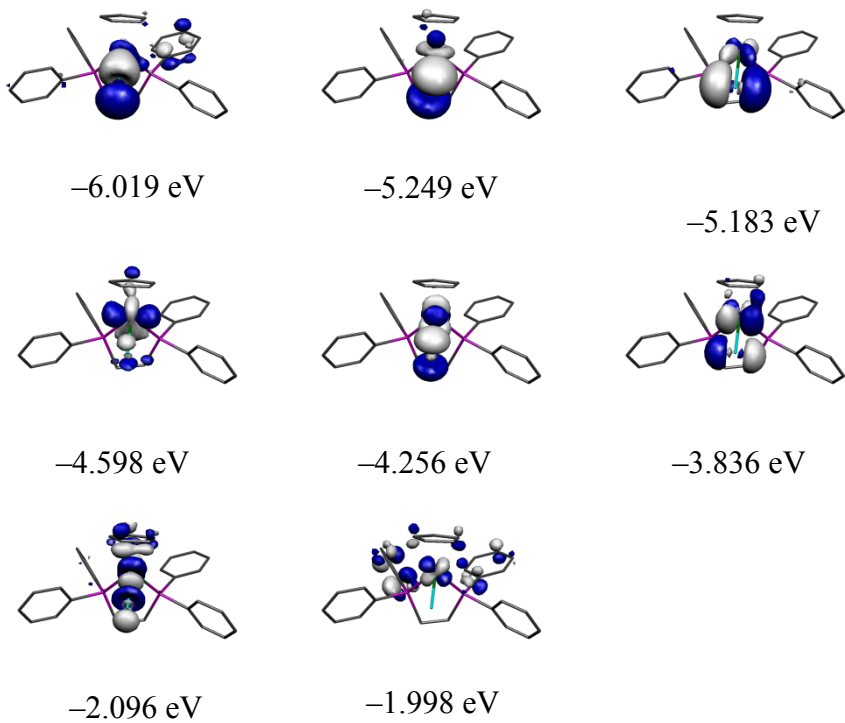
Kohn-Sham MO plots from HOMO-4 (top left) to LUMO+1 (bottom left)

**[Fe(Cp)(I)(dppe)], 1I**



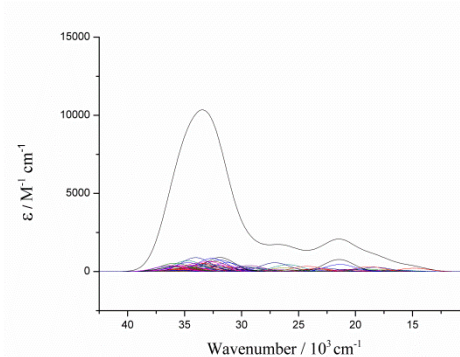
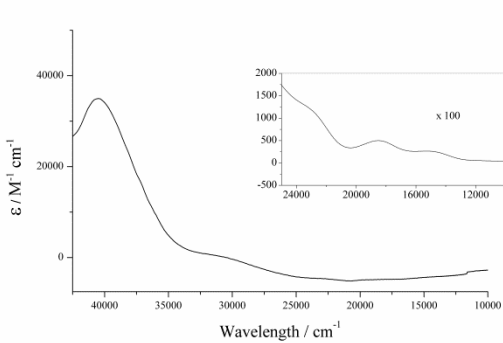
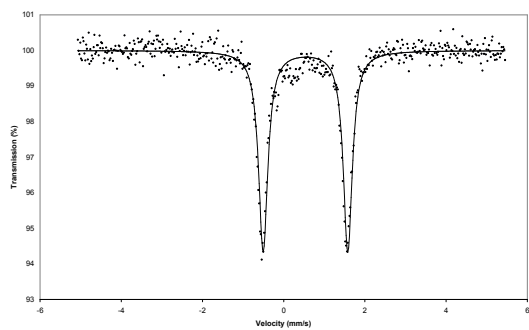
Top – Mossbauer

Bottom Left – Experimental UV-vis, Bottom Right – Calculated UV-vis



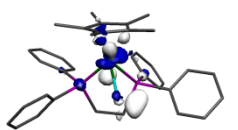
Kohn-Sham MO plots from HOMO-5 (top left) to LUMO+1 (bottom left)

**[Fe(Cp\*)(I)(dppe)], 2I**

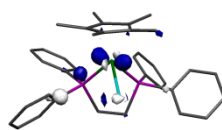


Top – Mossbauer

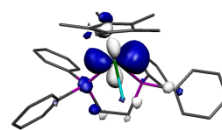
Bottom Left – Experimental UV-vis, Bottom Right – Calculated UV-vis



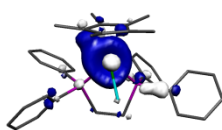
-5.074 eV



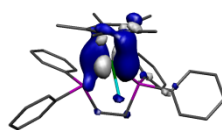
-4.991 eV



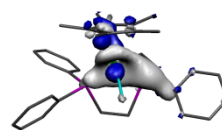
-4.311 eV



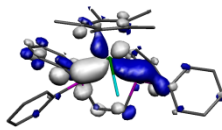
-3.958 eV



-3.625 eV



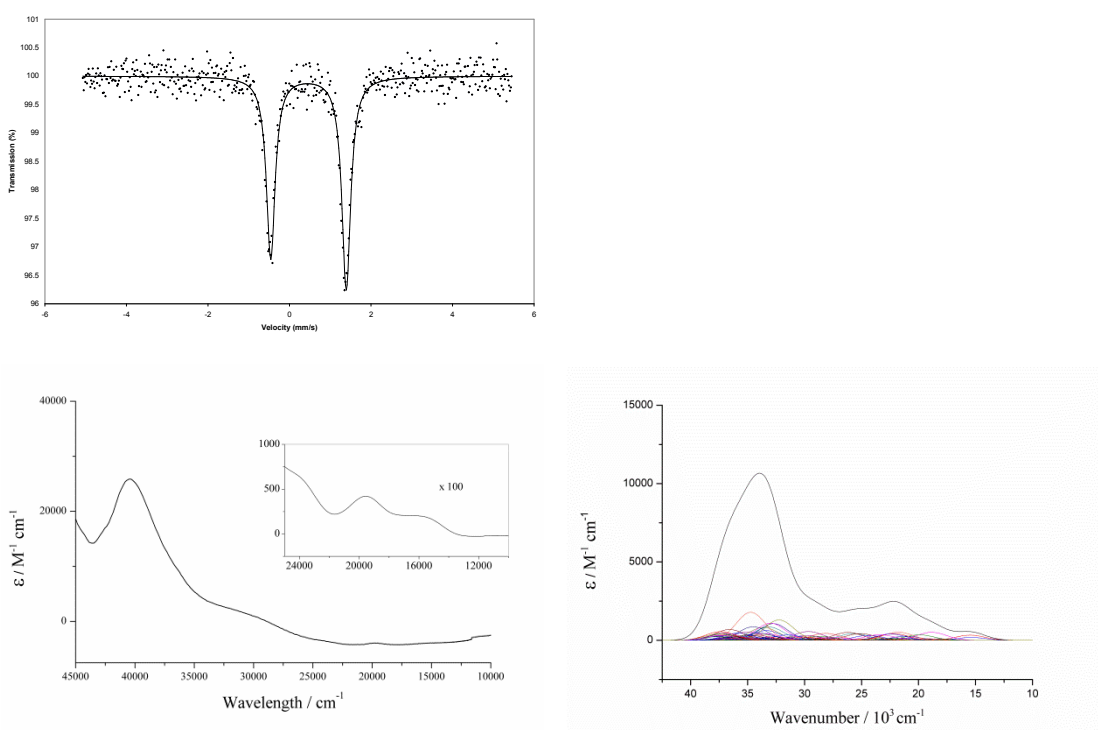
-1.996 eV



-1.819 eV

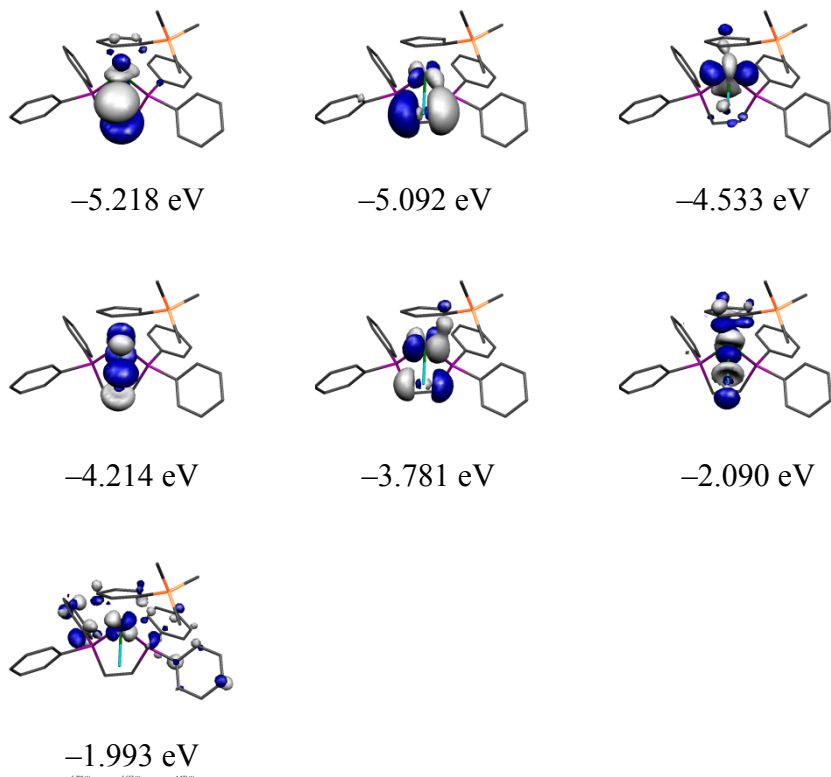
Kohn-Sham MO plots from HOMO-4 (top left) to LUMO+1 (bottom left)

**[Fe(Cp')(I)(dppe)], 3I**



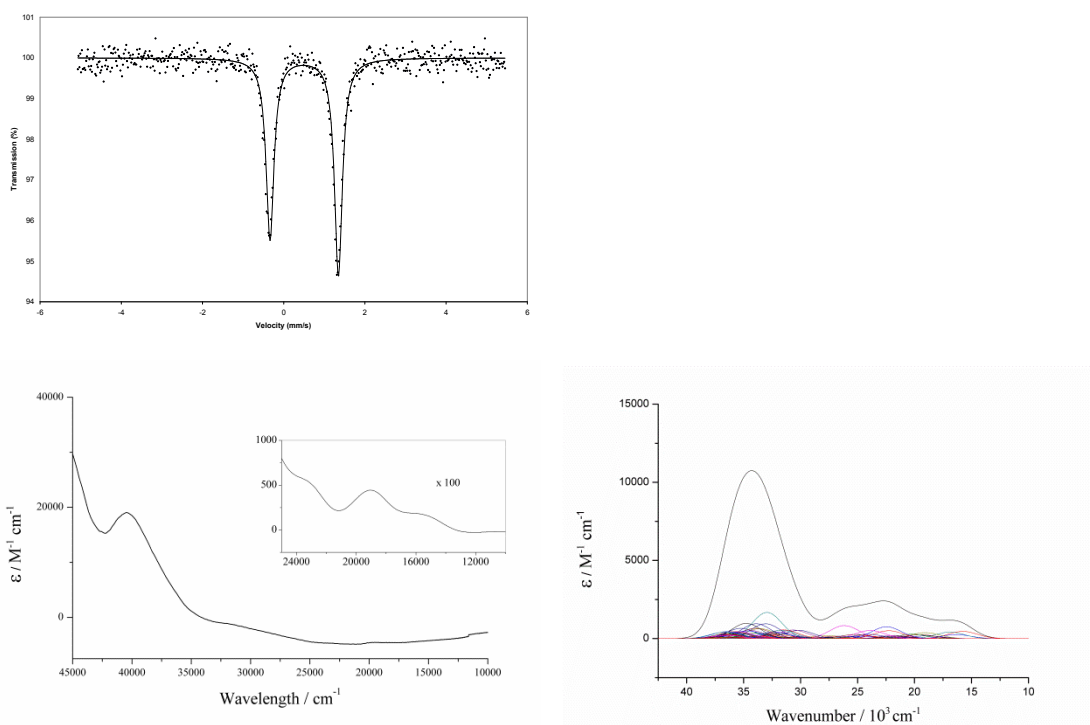
Top – Mossbauer

Bottom Left – Experimental UV-vis, Bottom Right – Calculated UV-vis



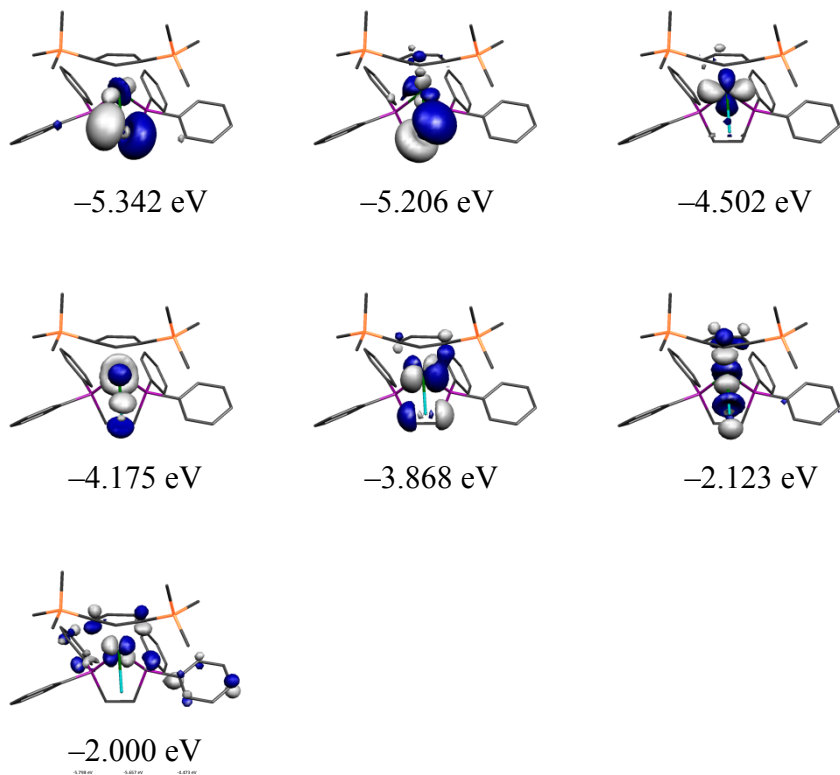
Kohn-Sham MO plots from HOMO-4 (top left) to LUMO+1 (bottom left)

**[Fe(Cp'')(I)(dppe)], 4I**



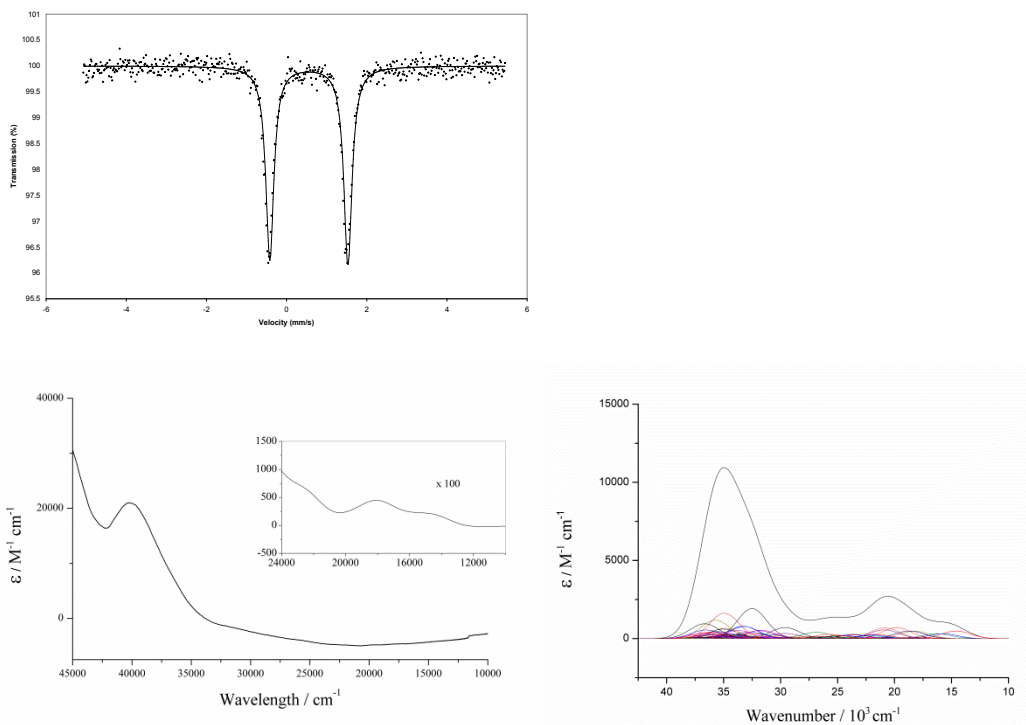
Top – Mossbauer

Bottom Left – Experimental UV-vis, Bottom Right Calculated UV-vis



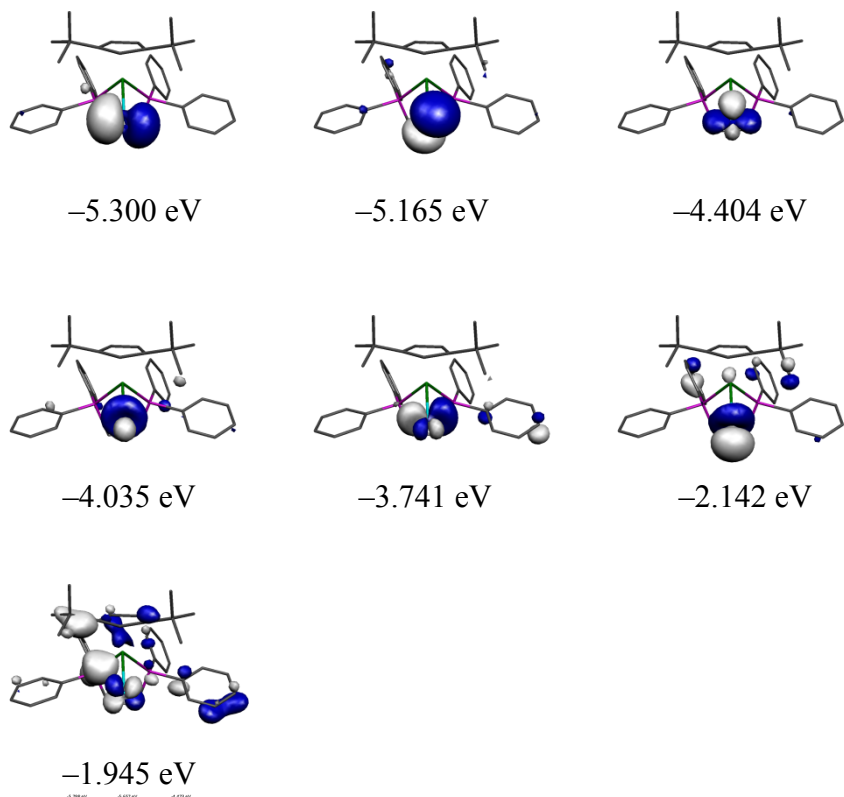
Kohn-Sham MO plots from HOMO-4 (top left) to LUMO+1 (bottom left)

**[Fe(Cp<sup>t</sup>)(I)(dppe)], 5I**



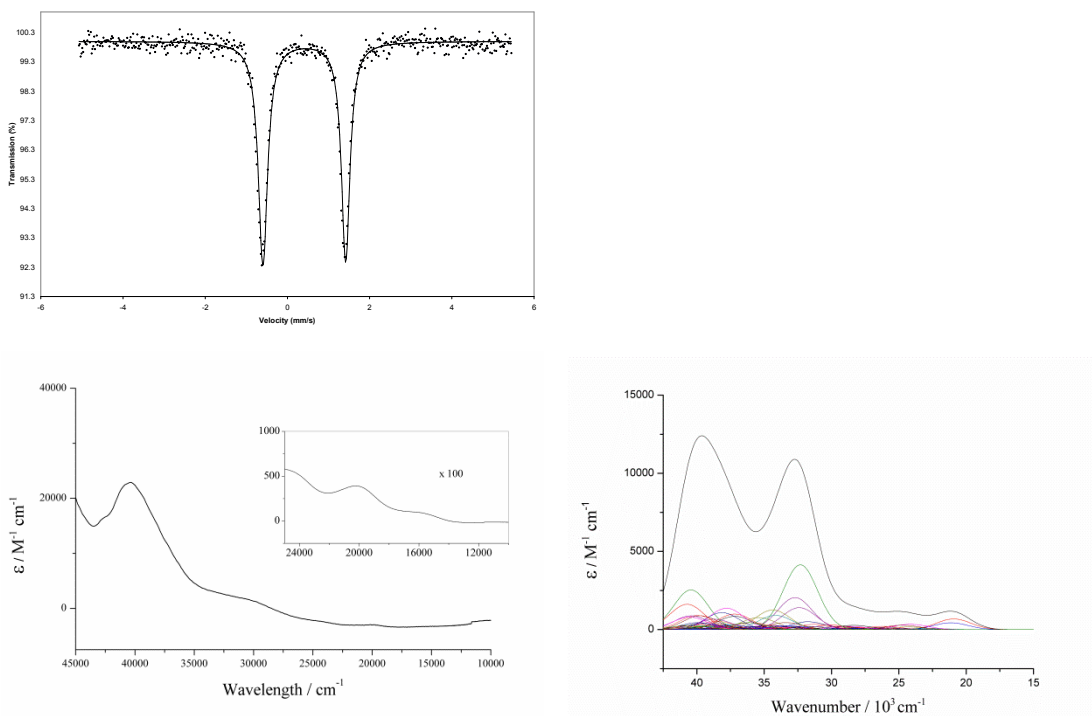
Top – Mossbauer

Bottom Left – Experimental UV-vis, Bottom Right – Calculated UV-vis



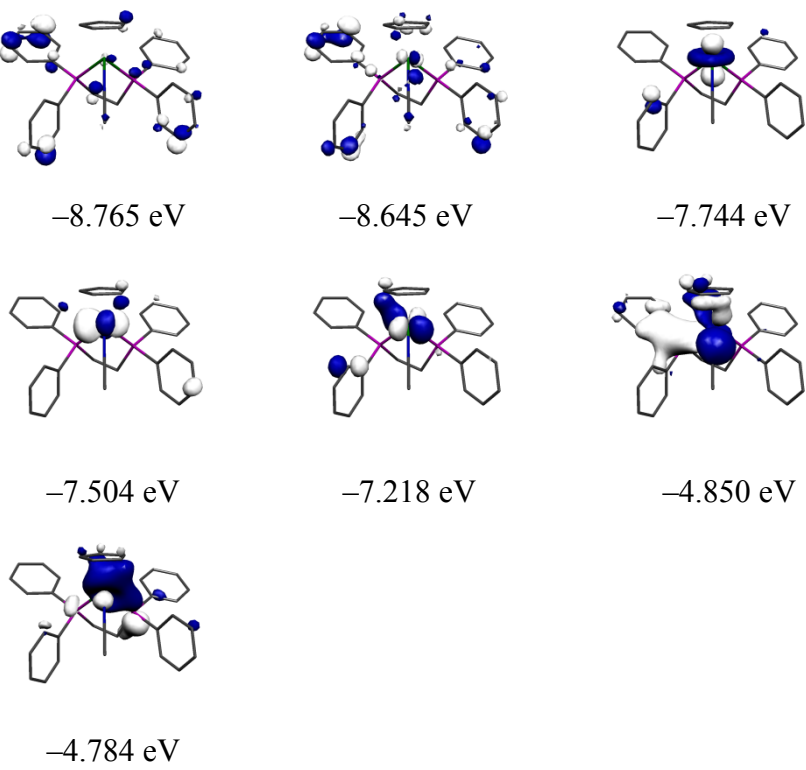
Kohn-Sham MO plots from HOMO-4 (top left) to LUMO+1 (bottom left)

**[Fe(Cp)(NCMe)(dppe)][I], 1SIP**



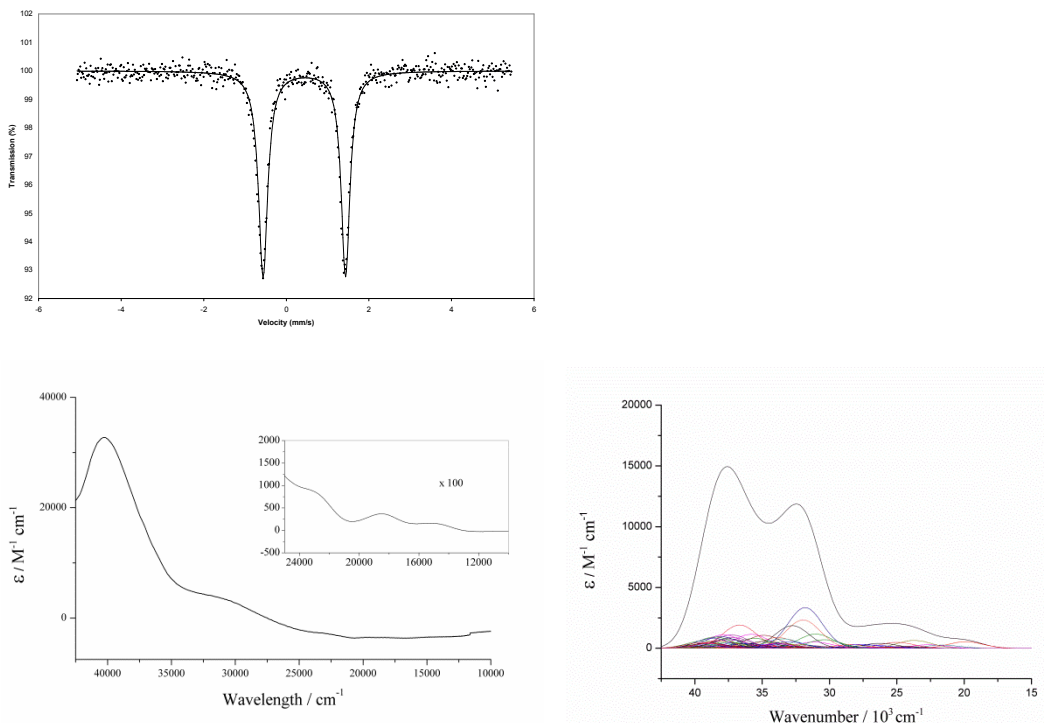
Top – Mossbauer

Bottom Left – Experimental UV-vis, Bottom Right – Calculated UV-vis



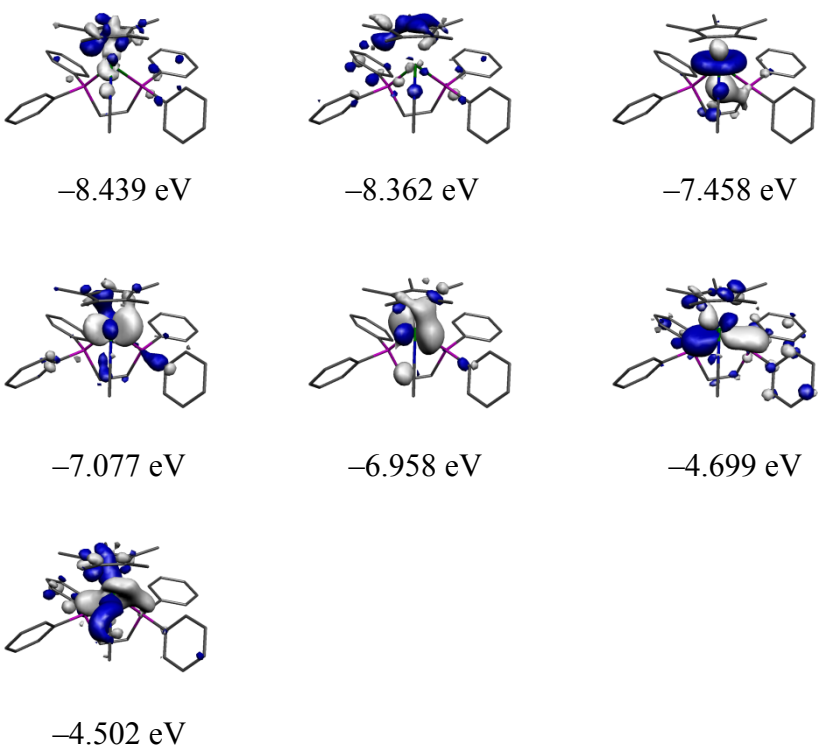
Kohn-Sham MO plots from HOMO-4 (top left) to LUMO+1 (bottom left)

**[Fe(Cp\*)(NCMe)(dppe)][I], 2SIP**



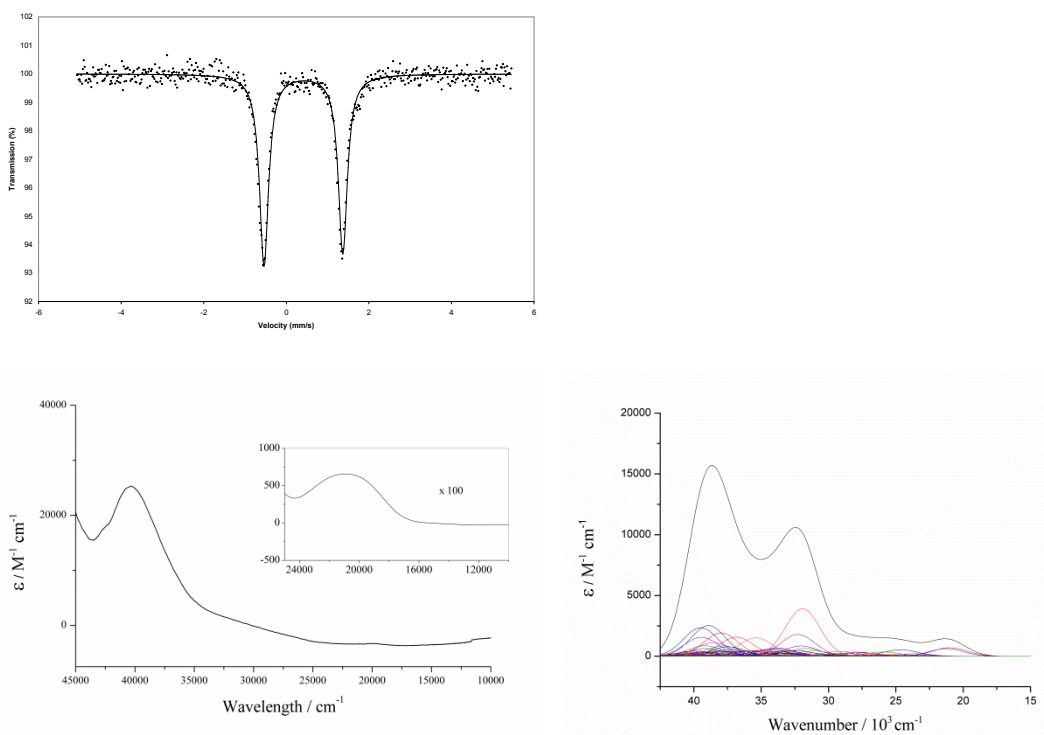
Top – Mossbauer

Bottom Left – Experimental UV-vis, Bottom Right – Calculated UV-vis



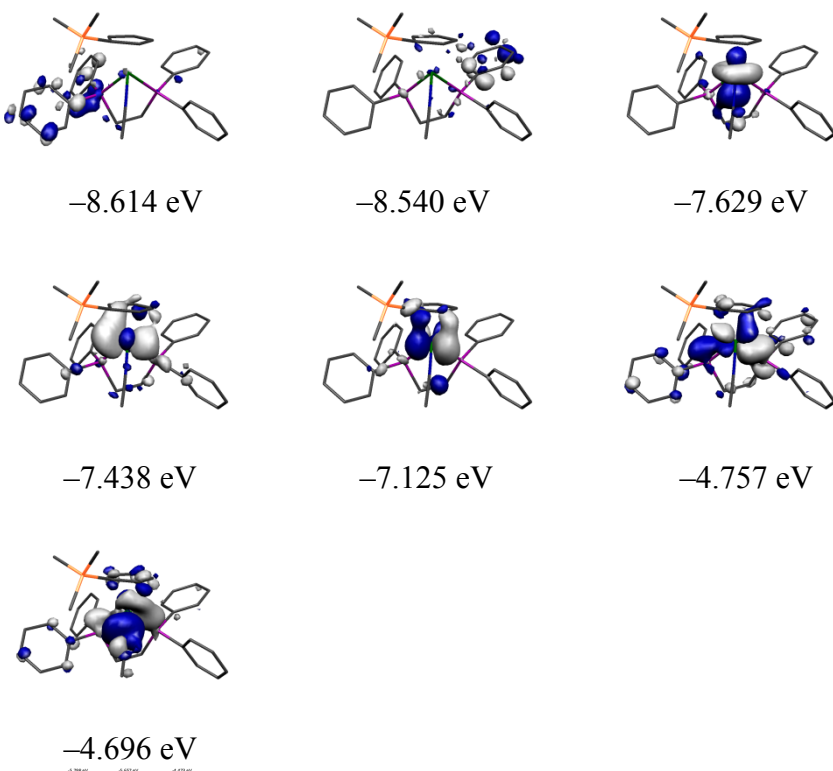
Kohn-Sham MO plots from HOMO-4 (top left) to LUMO+1 (bottom left)

**[Fe(Cp')(NCMe))(dppe)][I], 3SIP**



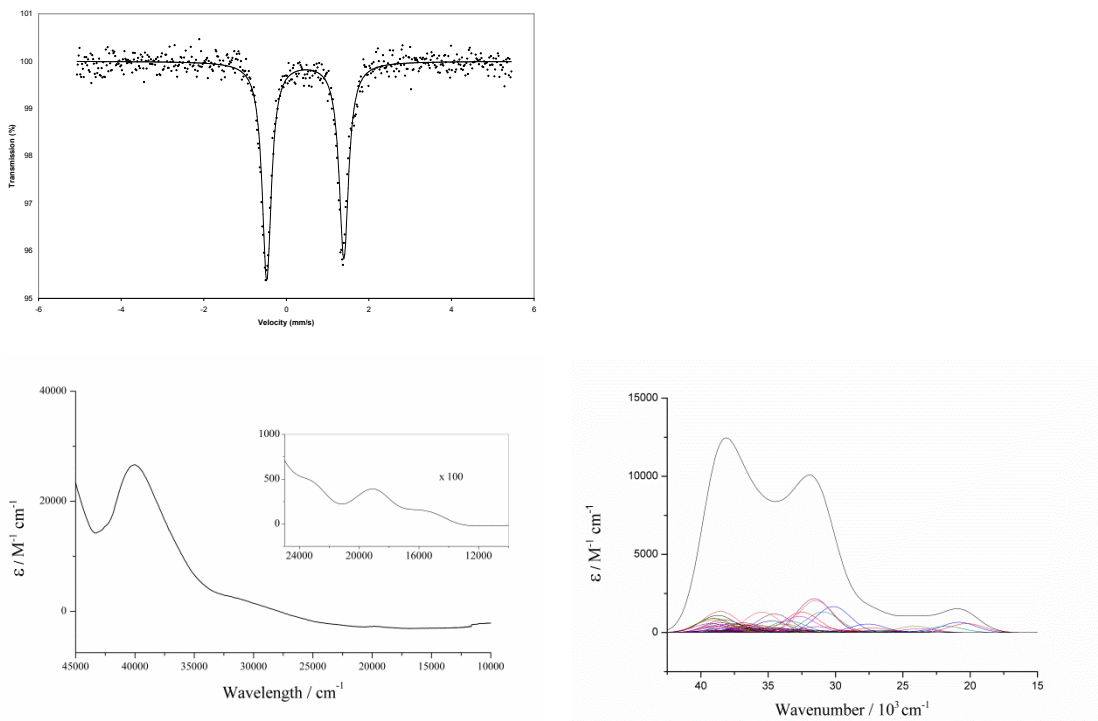
Top – Mossbauer

Bottom Left – Experimental UV-vis, Bottom Right – Calculated UV-vis



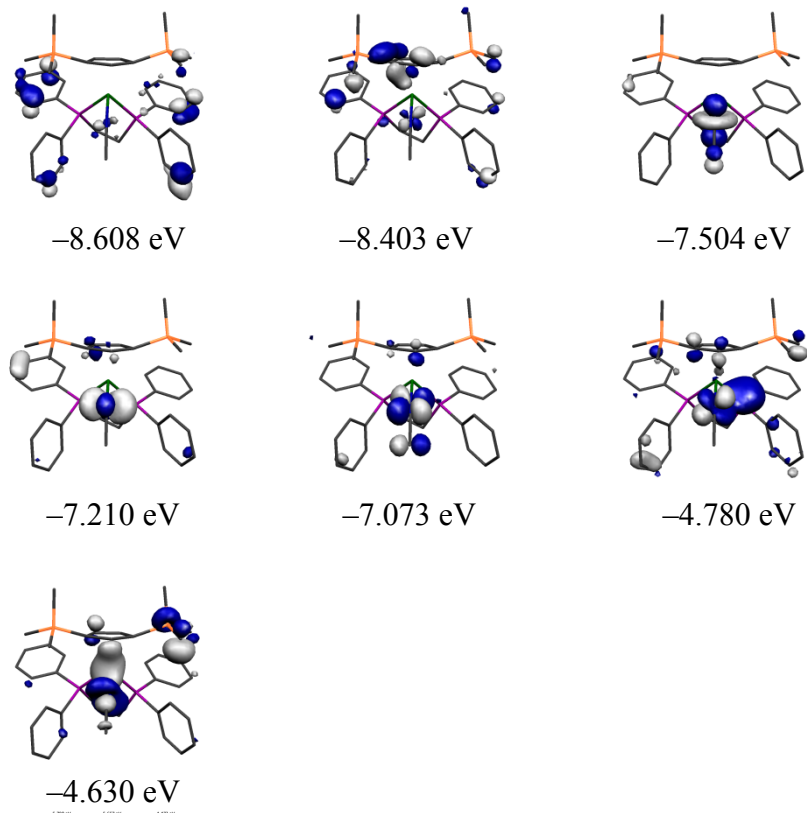
Kohn-Sham MO plots from HOMO-4 (top left) to LUMO+1 (bottom left)

**[Fe(Cp'')(NCMe)(dppe)][I], 4SIP**



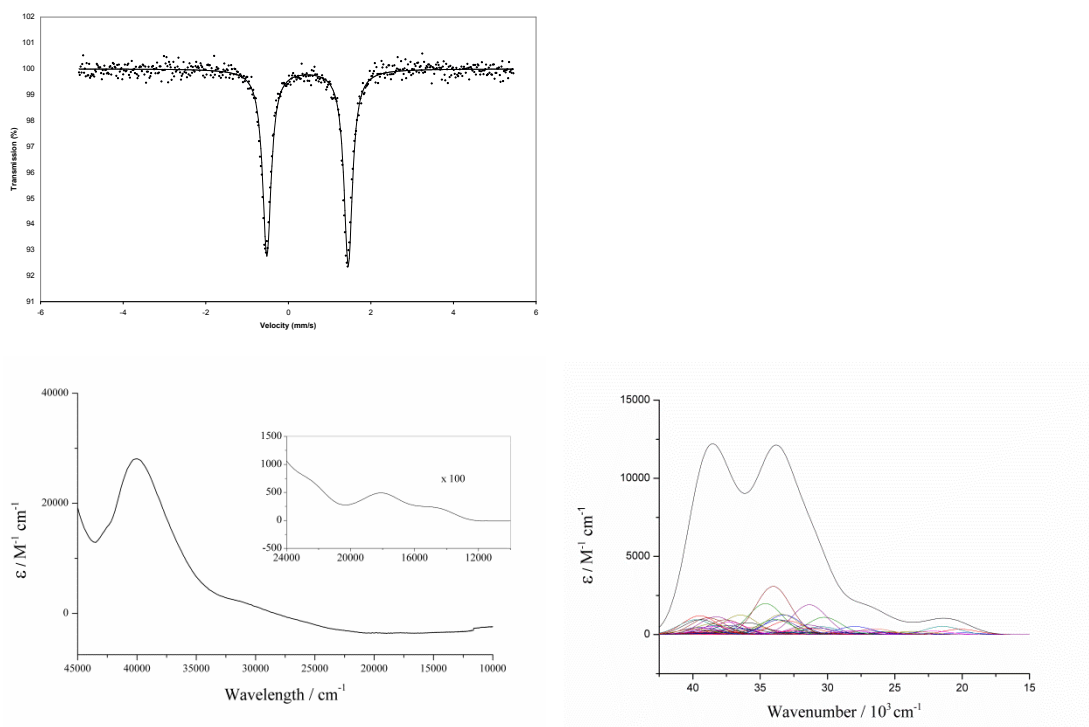
Top – Mossbauer

Bottom Left – Experimental UV-vis, Bottom Right – Calculated UV-vis



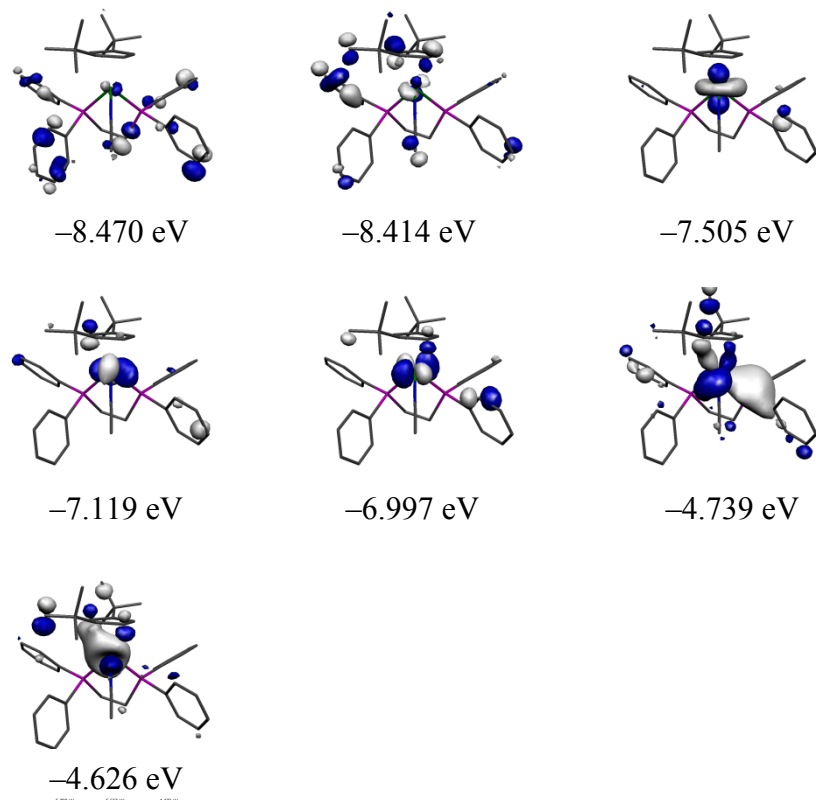
Kohn-Sham MO plots from HOMO-4 (top left) to LUMO+1 (bottom left)

**[Fe(Cp<sup>t</sup>)(NCMe)(dppe)][I], 5SIP**



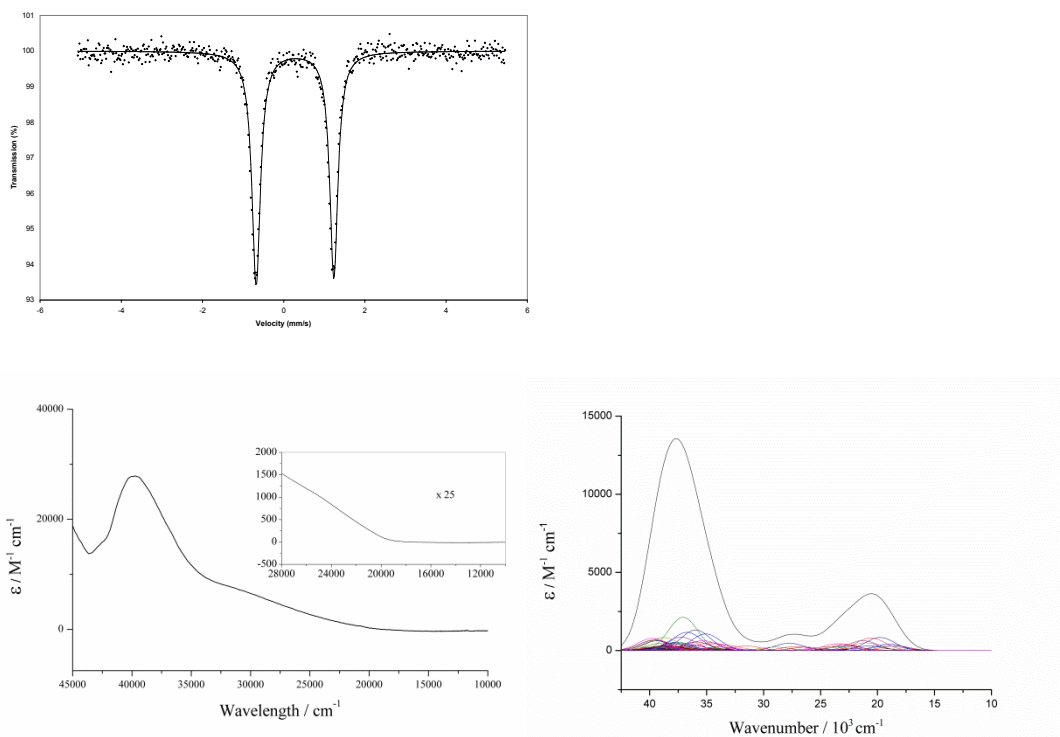
Top – Mossbauer

Bottom Left – Experimental UV-vis, Bottom Right – Calculated UV-vis



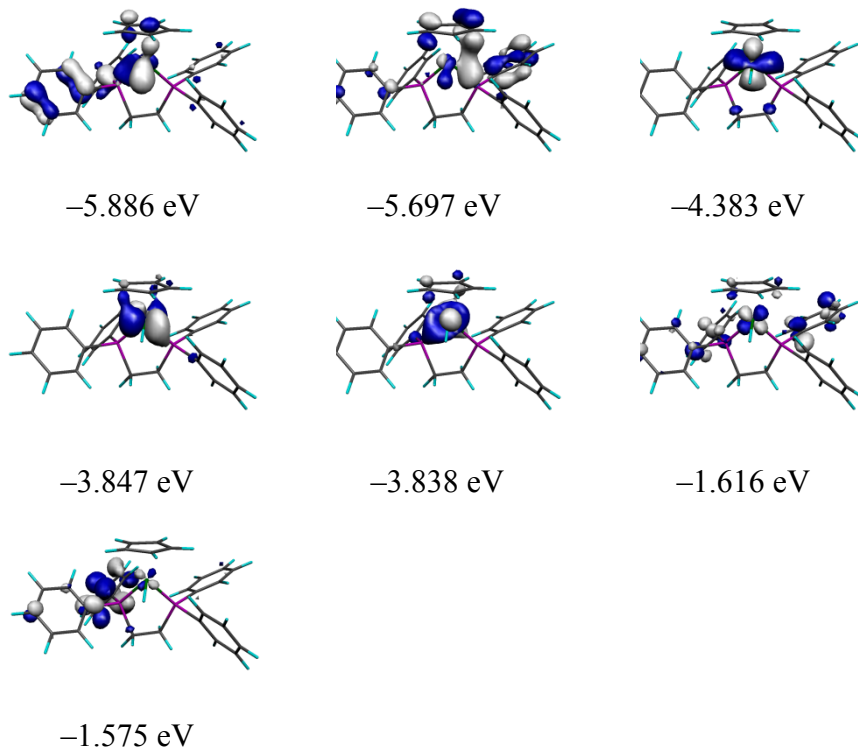
Kohn-Sham MO plots from HOMO-4 (top left) to LUMO+1 (bottom left)

[Fe(Cp)(H)(dppe)], 1H



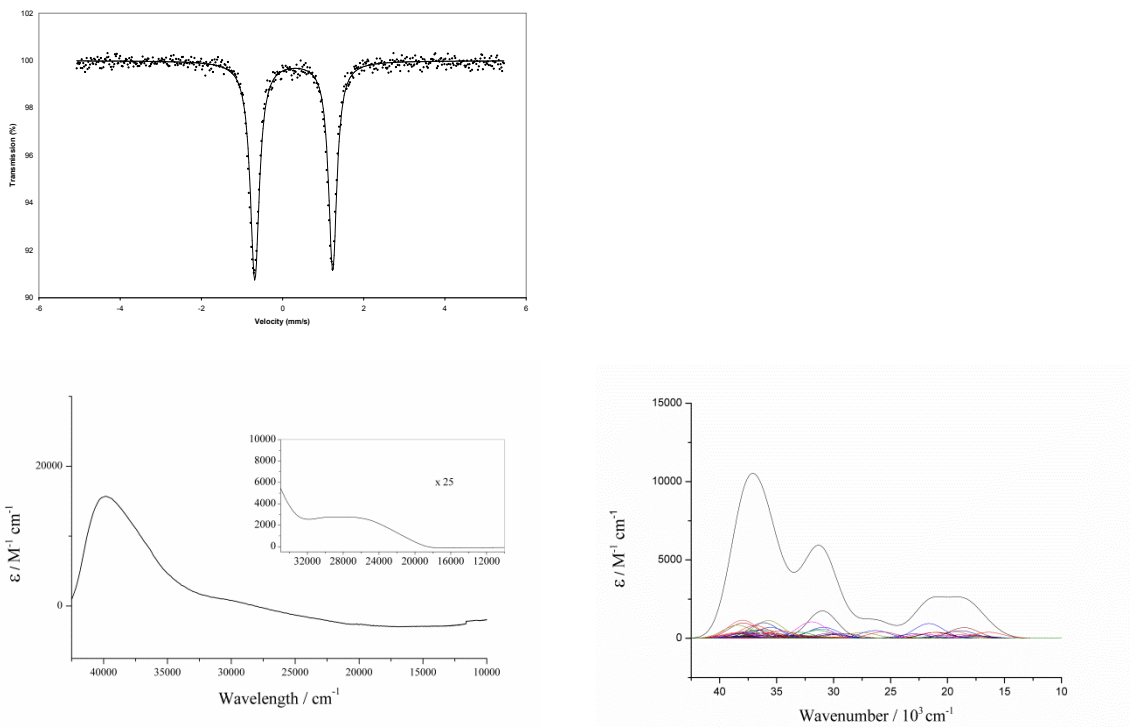
Top – Mossbauer

Bottom Left – Experimental UV-vis, Bottom Right – Calculated UV-vis



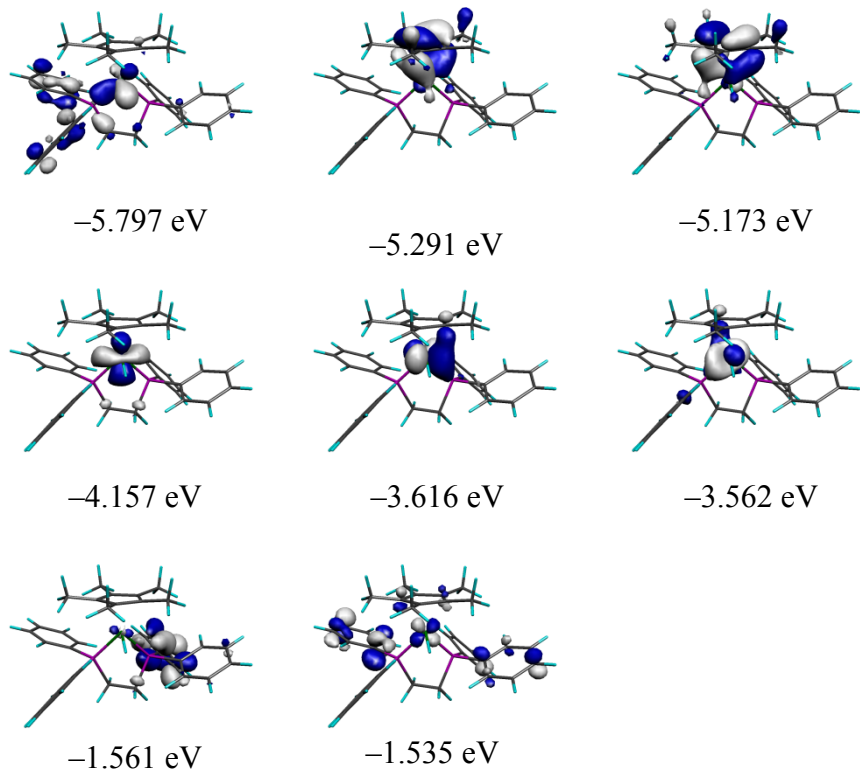
Kohn-Sham MO plots from HOMO-4 (top left) to LUMO+1 (bottom left)

**[Fe(Cp\*)(H)(dppe)], 2H**



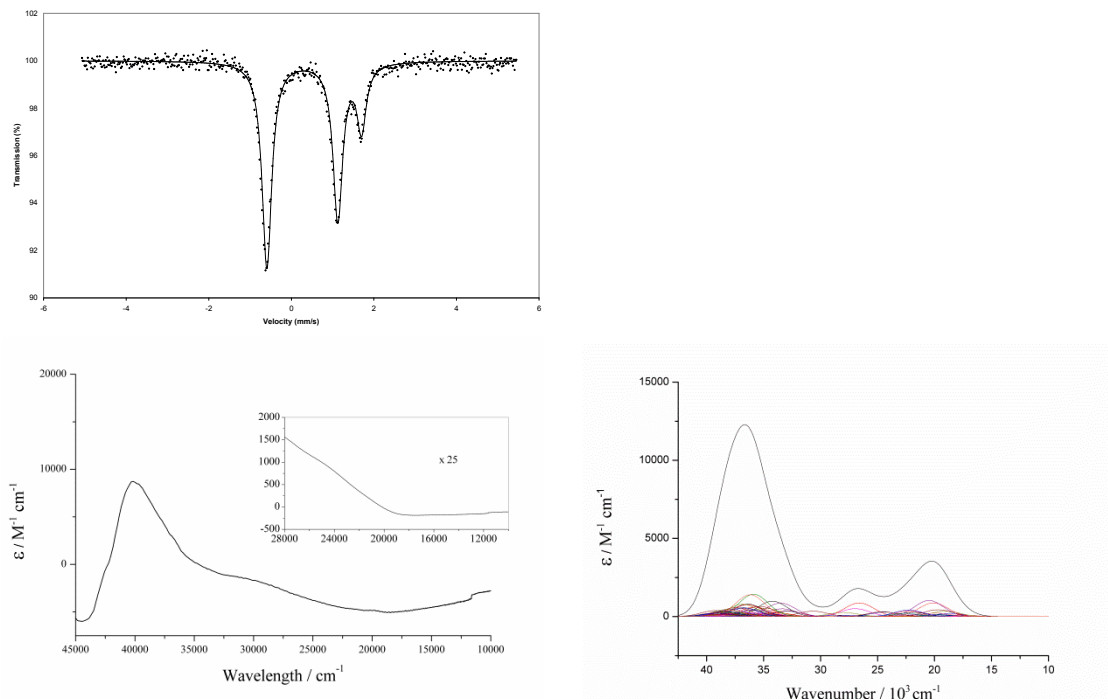
Top – Mossbauer

Bottom Left – Experimental UV-vis, Bottom Right – Calculated UV-vis



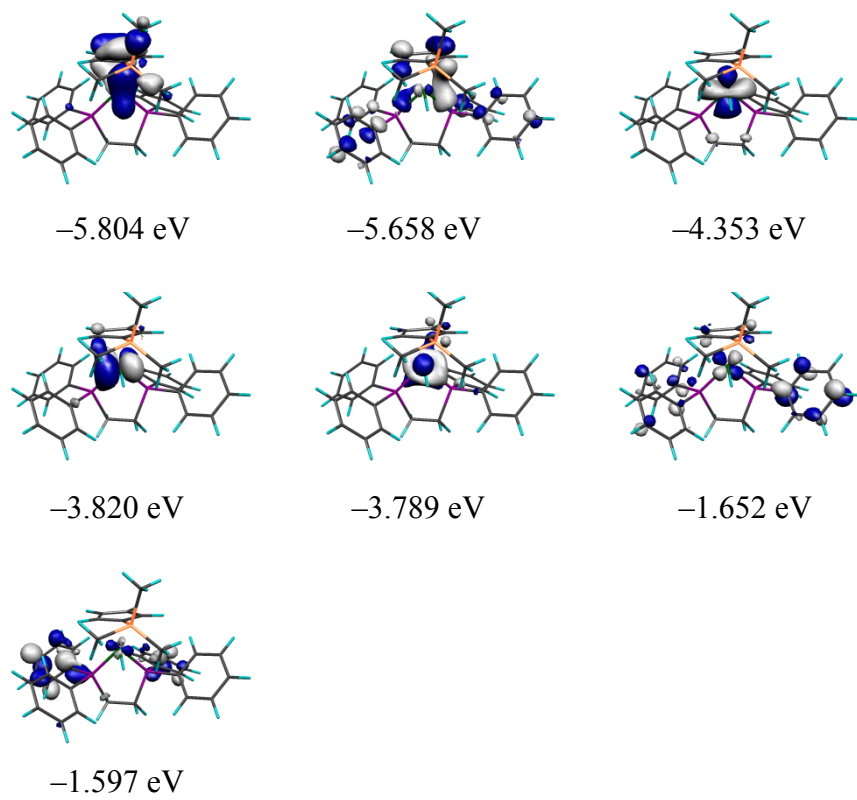
Kohn-Sham MO plots from HOMO-5 (top left) to LUMO+1 (bottom left)

**[Fe(Cp')(H)(dppe)], 3H**



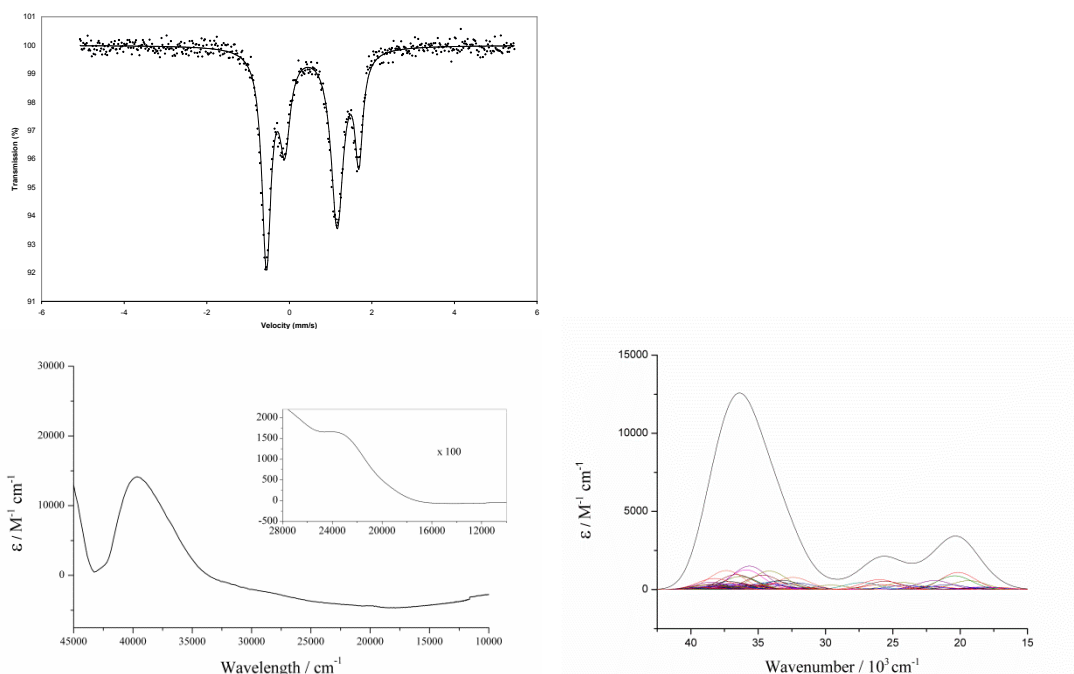
Top – Mossbauer. The Mössbauer spectrum of this compound showed two species, the major component is **3H** and the minor component is most likely a product of decomposition.

Bottom Left – Experimental UV-vis, Bottom Right – Calculated UV-vis



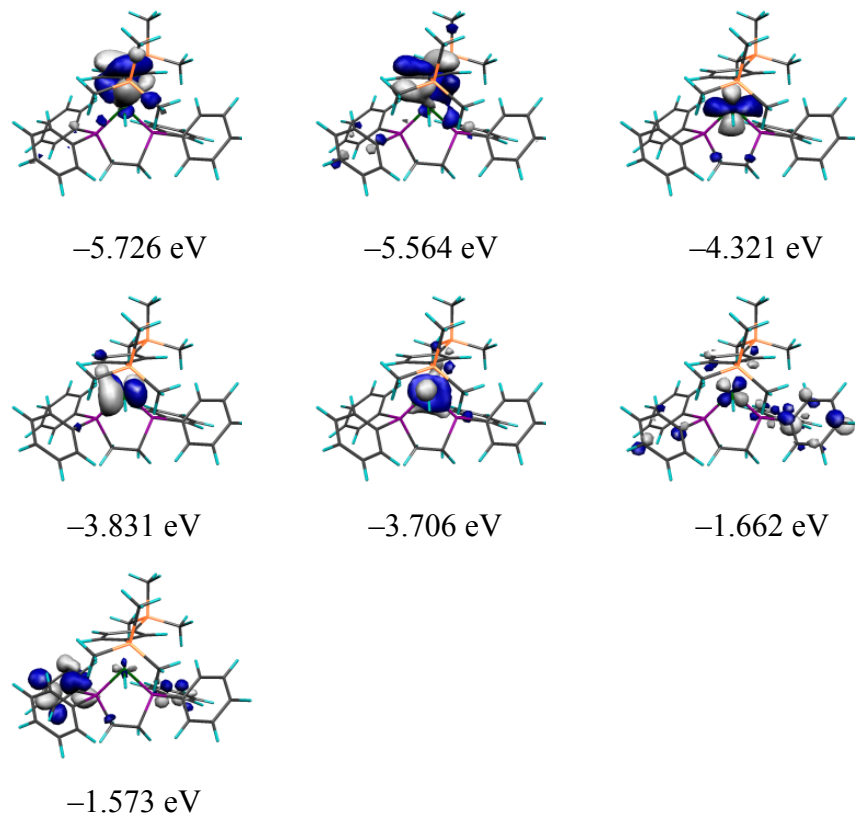
Kohn-Sham MO plots from HOMO-4 (top left) to LUMO+1 (bottom left)

**[Fe(Cp'')(H)(dppe)], 4H**



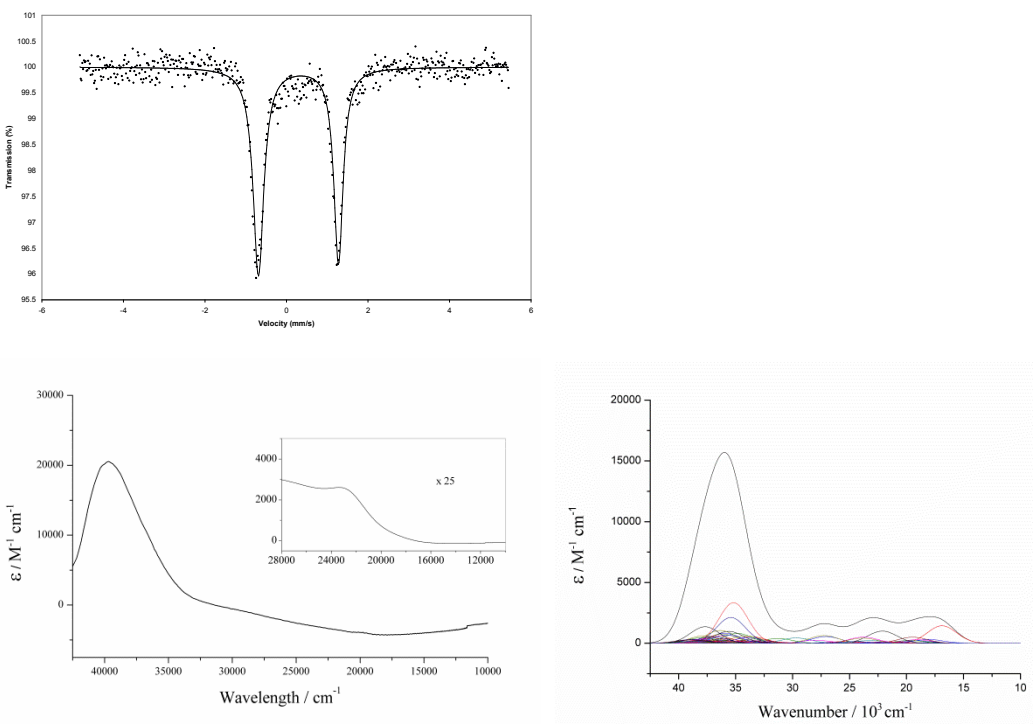
Top – Mossbauer. The Mössbauer spectrum of this compound showed two species, the major component is **4H** and the minor component is most likely a product of decomposition'

Bottom Left – Experimental UV-vis, Bottom Right – Calculated UV-vis



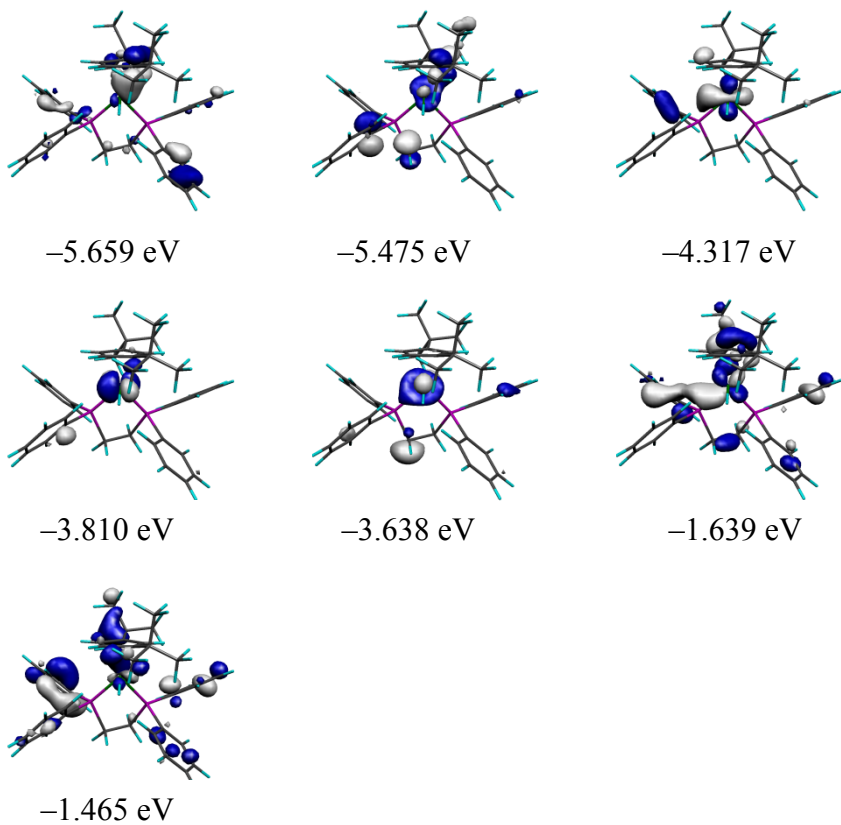
Kohn-Sham MO plots from HOMO-4 (top left) to LUMO+1 (bottom left)

**[Fe(Cp<sup>t</sup>)(H)(dppe)], 5H**



Top – Mossbauer

Bottom Left – Experimental UV-vis, Bottom Right – Calculated UV-vis



Kohn-Sham MO plots from HOMO-4 (top left) to LUMO+1 (bottom left)